ETSI TR 104 141 V1.1.1 (2026-03)

TECHNICAL REPORT

Practical Methods for Wireless Backhaul Planning with New KPIs

Reference
DTR/ATTMTMmWT-0031

Keywords
backhaul, BTA, microwave, millimetre wave,
new KPIs, wireless

ETSI

650 Route des Lucioles
F-06921 Sophia Antipolis Cedex - FRANCE

Tel.: +33 4 92 94 42 00 Fax: +33 4 93 65 47 16

Siret N° 348 623 562 00017 - APE 7112B
Association à but non lucratif enregistrée à la
Sous-Préfecture de Grasse (06) N° w061004871

Contents

Intellectual Property Rights

Essential patents

IPRs essential or potentially essential to normative deliverables may have been declared to ETSI. The declarations pertaining to these essential IPRs, if any, are publicly available for **ETSI members and non-members**, and can be found in ETSI SR 000 314: *"Intellectual Property Rights (IPRs); Essential, or potentially Essential, IPRs notified to ETSI in respect of ETSI standards"*, which is available from the ETSI Secretariat. Latest updates are available on the ETSI IPR online database.

Pursuant to the ETSI Directives including the ETSI IPR Policy, no investigation regarding the essentiality of IPRs, including IPR searches, has been carried out by ETSI. No guarantee can be given as to the existence of other IPRs not referenced in ETSI SR 000 314 (or the updates on the ETSI Web server) which are, or may be, or may become, essential to the present document.

Trademarks

The present document may include trademarks and/or tradenames which are asserted and/or registered by their owners. ETSI claims no ownership of these except for any which are indicated as being the property of ETSI, and conveys no right to use or reproduce any trademark and/or tradename. Mention of those trademarks in the present document does not constitute an endorsement by ETSI of products, services or organizations associated with those trademarks.

DECT™, **PLUGTESTS™**, **UMTS™** and the ETSI logo are trademarks of ETSI registered for the benefit of its Members. **3GPP™**, **LTE™** and **5G™** logo are trademarks of ETSI registered for the benefit of its Members and of the 3GPP Organizational Partners. **oneM2M™** logo is a trademark of ETSI registered for the benefit of its Members and of the oneM2M Partners. **GSM®** and the GSM logo are trademarks registered and owned by the GSM Association.

Foreword

This Technical Report (TR) has been produced by ETSI Technical Committee Access, Terminals, Transmission and Multiplexing (ATTM).

Modal verbs terminology

In the present document "**should**", "**should not**", "**may**", "**need not**", "**will**", "**will not**", "**can**" and "**cannot**" are to be interpreted as described in clause 3.2 of the ETSI Drafting Rules (Verbal forms for the expression of provisions).

"**must**" and "**must not**" are **NOT** allowed in ETSI deliverables except when used in direct citation.

Executive summary

The Radio Fixed Services community represented by the ETSI ATTM TM_mWT Working Group has recently defined an innovative planning methodology for wireless backhaul links with the key benefit of enabling a cost-effective network design by reducing the required system margins in most microwave and millimetre-wave transport scenarios, compared to the current criteria, with negligible impact on the end-to-end Quality of Experience (QoE) of the Radio Access Network (RAN) users.

The novel planning methodology (that will be also referred to as the "New KPIs methodology" in the present document) reformulates the definition of two indicators already in use in current backhaul networks design - namely, the Peak Information Rate (PIR) and the Committed Information Rate (CIR) - and introduces the Backhaul Traffic Availability (BTA) as an innovative metric to assess the link performance by accounting for traffic-related information.

While on the one hand the BTA provides an effective representation of the probability that any backhaul link does not cause congestion in the aggregated RAN data flows, on the other hand it requires to operatively choose a specific traffic demand distribution to complete the assessment, thus possibly limiting the immediacy and in some cases the practical applicability of the New KPIs approach.

The present document takes up the challenge to overcome this hindrance by proposing practical methods to make the assessment of the BTA an immediate and straightforward process, once few baseline features of the target backhaul scenario are known. As a first key contribution, an experimentally validated analytical procedure for deriving the lower bound of the BTA of any given backhaul link with unknown traffic demand distribution - that can be readily employed for a conservative (i.e. worst-case) network planning - is disclosed. This method has the strategic advantage of relying on the only knowledge of the average and the peak values of the traffic demand envisioned for the link under investigation, thus making the choice of the complete statistical throughput distribution needed for computing the BTA metric a completely transparent process for the end user. Furthermore, the proposed procedure is conceived to be easily integrated into the software framework of the currently available backhaul planning tools, with the ultimate goal of further promoting and accelerating the adoption of the novel design paradigm in present and next generation transport networks.

As a second contribution, the present document describes a methodology for conducting measurement campaigns on live backhaul links with the aim of deriving a dataset of traffic demand distributions to be possibly used as reference statistics for the assessment of the BTA at least in a group of significant transport scenarios. In this context, the results of an experimental activity carried out during the preparation of the present document are also disclosed, serving as an example of how the proposed guidelines can be applied to build a proprietary database of backhaul traffic statistics to be employed in the network design process.

Finally, a comprehensive planning procedure for an illustrative point-to-point E-band link developed in accordance with the whole New KPIs paradigm is presented in order to provide a practical guide that can be adapted and scaled to more complex network scenarios and configurations.

Introduction

The projected traffic volumes driven by the proliferation of 5G and Beyond Radio Access Technologies (RATs) have raised serious concerns regarding the economic sustainability of transport infrastructures, particularly with respect to the Total Cost of Ownership (TCO). In this context, enhancing the cost efficiency of wireless networks by reducing the system margins often introduced by potentially over-engineered design methods has become imperative for telecom operators.

The Radio Fixed Services community represented by the ETSI ATTM TM_mWT Working Group has recently devoted significant efforts in this direction by finally defining an innovative planning methodology for wireless backhaul links in ETSI GR mWT 028 [i.1]. This new approach has been shown to lead to the key benefit of enabling a cost-effective network design by limiting the required system margins in most microwave and millimetre-wave transport scenarios, compared to the current criteria, with negligible impact on the end-to-end Quality of Experience (QoE) of the Radio Access Network (RAN) users.

The novel planning methodology (that will be also referred to in the following of the present document as the "New KPIs methodology") reformulates the definition of two indicators already in use in current backhaul networks design - namely, the Peak Information Rate (PIR) and the Committed Information Rate (CIR) - and introduces the Backhaul Traffic Availability (BTA) as an innovative metric to assess the link performance by accounting for traffic-related information. More specifically:

- The PIR is still defined as the maximum theoretical traffic that can be generated by the ensemble of the RAT layers transported over a given backhaul link, and it can be readily computed according to the well-established guidelines in, e.g., NGMN 0.4.2 [i.2] (figure 1 provides an overview of possible methods for the case of a single RAN site with three sectors). Unlike the current planning approach for backhaul networks, the New KPIs methodology does not associate the PIR with any availability requirement. Instead, it is dimensioned using a practical system-level criterion by adopting a fade margin of 5 dB to 10 dB to ensure stable link operation.

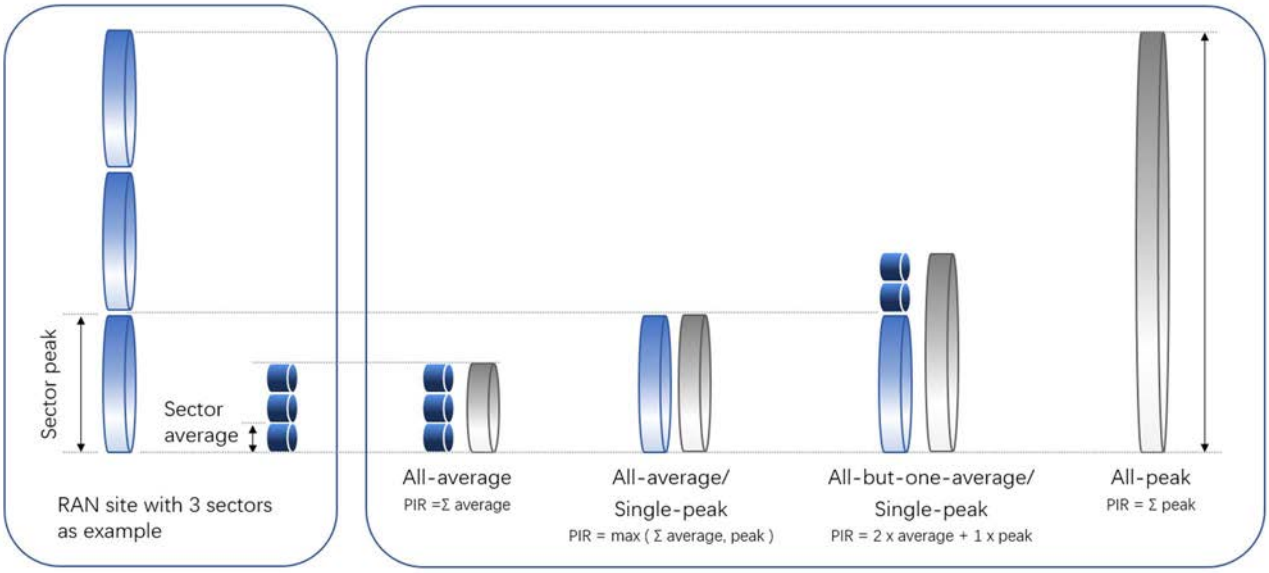

Figure 1: Overview of current methods for estimating the PIR for the case of a single RAN site with three sectors

- The CIR is recommended to be tailored to the minimum amount of capacity exclusively targeted to guarantee the survivability of the RAN and the essential and operator-specific top-priority services for the maximum time in a year (i.e. with an availability higher than 99,99 %).

  While the amount of traffic required to meet the first objective can be easily calculated for the different RATs - since it corresponds to the necessary information flows to transfer the control, management and synchronization planes to the base stations - top-priority services are more difficult to quantify as they mostly depend on the specific propositions of Mobile Network Operators (MNOs) for their own customers and could comprise voice traffic (including emergency calls), Guaranteed Bit Rate (GBR) applications (e.g. mission-critical voice/video, real-time streams and 5G new use cases), as well as Service Level Agreement (SLA) data sessions. In any case, it is important to emphasize that the target CIR values to be employed in the novel wireless backhaul planning approach are highly dependent on the specific RAT scenarios, and they cannot be blindly estimated as a fixed percentage of the PIR across all cases. For example, in standalone 5G or mixed 4G and 5G sites baseline CIRs should be configured to fall between 1 % and 2 % of the PIR - significantly lower than the 10 % to 20 % range usually considered in current design methodologies (see ETSI GR mWT 028 [i.1] for a more detailed analysis on this matter).

- The BTA is defined as the probability that a given backhaul link is capable to deliver the entire aggregated traffic demand with no impacts on the RAN end-users QoE and, under a mathematical standpoint, it is expressed by the following weighted sum:

$$BTA = \sum_{i=1}^{M} P(C_{BH}^{(i-1)} < T \leq C_{BH}^{(i)}) \times \vartheta_{BH}^{(i)}, \quad (1)$$

  where M is the total number of backhaul capacities that can be delivered, $\vartheta_{BH}^{(i)}$ represents the availability of the ith backhaul capacity $C_{BH}^{(i)}$ (with $C_{BH}^{(1)} < C_{BH}^{(2)} < \ldots < C_{BH}^{(M)}$), and $P\left(C_{BH}^{(i-1)} < T \leq C_{BH}^{(i)}\right)$ denotes the probability that the aggregated traffic demand T lies in the range between $C_{BH}^{(i-1)}$ and $C_{BH}^{(i)}$, being $C_{BH}^{(0)} = 0$ bit/s the link failure state. Terms $\vartheta_{BH}^{(i)}$ can be derived by applying the well-established guidelines and methods described in Recommendation ITU-R P.530-19 [i.4] and references therein, while probabilities $P\left(C_{BH}^{(i-1)} < T \leq C_{BH}^{(i)}\right)$ can be easily computed from the cumulative distribution function $F_T(t)$ of the link aggregated traffic demand as (with $i = 1,2, \ldots, M$):

$$P\left(C_{BH}^{(i-1)} < T \leq C_{BH}^{(i)}\right) = F_T\left(C_{BH}^{(i)}\right) - F_T\left(C_{BH}^{(i-1)}\right) \quad (1a)$$

A massive number of system-level simulations accounting for different network conditions and aggregated RAN traffic demand profiles carried out in ETSI GR mWT 028 [i.1] have demonstrated that wireless backhaul links with BTA values above the 99,7 % to 99,9 % range do not introduce any perceivable degradation in the average end-to-end QoE performance of the RAN users even under highly demanding application scenarios.

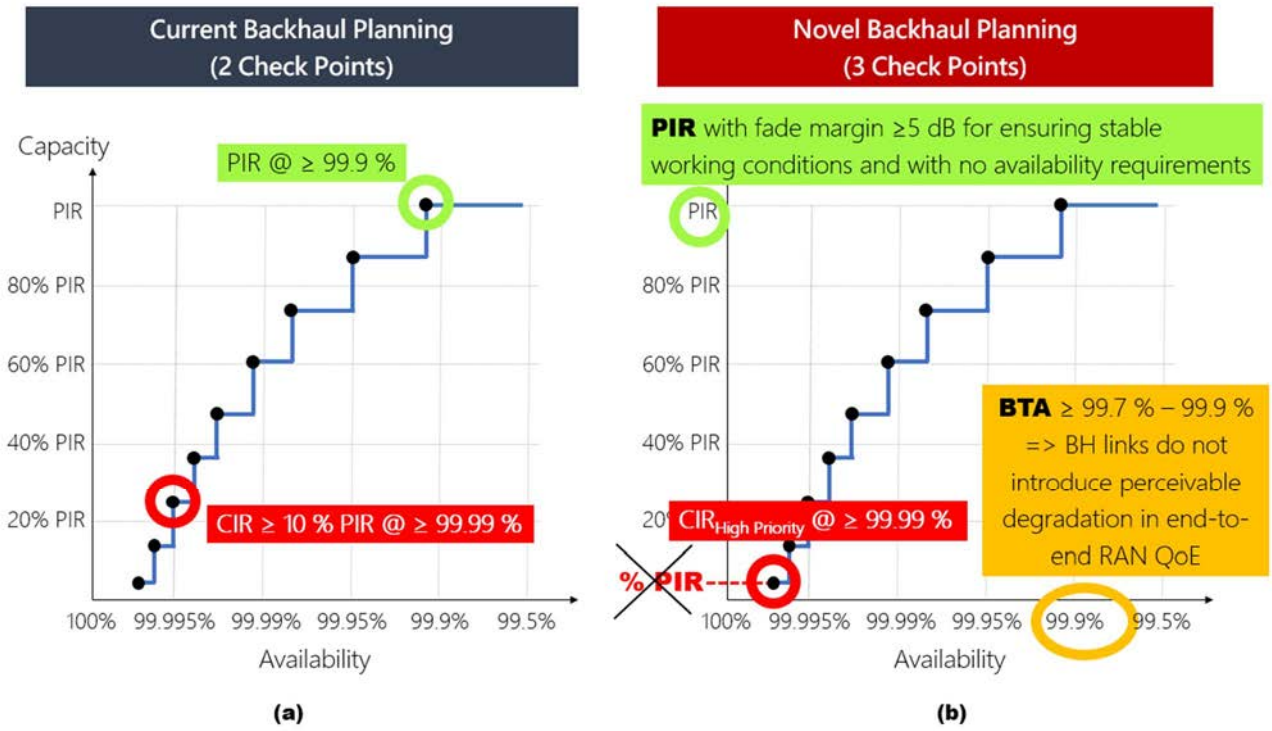

Figure 2: A comparison between current and novel planning methodologies for wireless backhaul links

The three check points characterizing the novel backhaul planning methodology described above are summarized in figure 2, that also presents a comparison with the current design approach.

On the one hand, the BTA offers an effective means of representing the probability that a given backhaul link does not cause congestion in the aggregated RAN data flows. On the other hand, though, it requires to operatively choose a specific traffic demand distribution to complete the assessment (i.e. for computing probabilities $P(C_{BH}^{(i-1)} < T \leq C_{BH}^{(i)})$ in equation (1)), thus possibly limiting the immediacy and in some cases the practical applicability of this approach, ultimately leading to a potential reluctance among MNOs to adopt the New KPIs methodology.

The present document takes up the challenge to overcome this hindrance by proposing practical methods for enabling a fast and straightforward assessment of the BTA, based solely on few baseline features of the target backhaul scenario. As a first key contribution, clause 4 discloses an experimentally validated analytical procedure for deriving the lower bound of the BTA of any given backhaul link on the basis of the sole knowledge of its average and peak expected aggregated traffic demands. The proposed approach offers the key benefit of leading to the derivation of a worst-case (i.e. minimum achievable) BTA value that does not depend on any specific assumption on the actual and complete traffic statistical distribution characterizing the link under inspection, and that can be readily employed for a conservative and effective network planning.

NOTE: It is remarked that, both in the last sentence and in similar contexts throughout the entire present document, the term "conservative" refers exclusively to the BTA evaluation. It does not extend to the overall New KPIs methodology, which is instead specifically designed to avoid introducing unnecessary system margins compared to current backhaul planning approaches.

As a second contribution, clause 5 describes a methodology for conducting measurement campaigns on live transport networks with the aim of generating a dataset of traffic demand distributions that can serve as reference statistics for the assessment of the BTA at least in a group of representative backhaul scenarios. In this context, the results of an experimental activity carried out during the preparation of the present document are also disclosed as a practical example of how to apply the proposed guidelines.

The use of the above-mentioned strategies for assessing the BTA is then exemplified in clause 6, that is entirely devoted to the description of a comprehensive planning procedure of a point-to-point link operating in E-band according to the whole New KPIs approach.

Finally, annex B presents a methodology targeted at a general assessment of the benefits, in terms of cost of ownership, of the New KPIs paradigm, with the ultimate goal of encouraging and accelerating its adoption in current and next-generation wireless backhaul networks.

1 Scope

The present document has the goal of defining practical and effective methods for planning wireless backhaul links according to the novel approach detailed in ETSI GR mWT 028 [i.1]. One key area of investigation and contribution is the design of appropriate prediction models of the aggregated traffic demand statistics of any backhaul link as a function of few high-level and easy-to-know RAN-related behavioural features, such as the average and the peak values of the transported throughput, or the configuration of the various radio access technologies implemented in the connected sites. The derived prediction models are conceived with the goal of being easily embedded within the software framework of the currently available backhaul planning tools, thus pursuing the strategic benefit of making the choice of the link traffic demand distribution required for enabling the New KPIs methodology (namely, for computing the BTA metric) a completely transparent process for the end user.

In this context, the present document discloses an analytical procedure targeted at deriving a pessimistic estimation of the BTA of any backhaul link on the basis of the sole knowledge of the average and the peak values of its traffic demand, that could be used for a conservative and practical network planning. Secondly, the present document describes a methodology for conducting measurement campaigns on live transport networks and for processing the collected data in order to create a discrete set of reference throughput demand distributions to be used in the assessment of the BTA of any backhaul link, after a proper identification and classification of its main deployment features (e.g. number and type of transported radio access layers) and statistical properties.

2 References

2.1 Normative references

Normative references are not applicable in the present document.

2.2 Informative references

References are either specific (identified by date of publication and/or edition number or version number) or non-specific. For specific references, only the cited version applies. For non-specific references, the latest version of the referenced document (including any amendments) applies.

NOTE: While any hyperlinks included in this clause were valid at the time of publication ETSI cannot guarantee their long-term validity.

The following referenced documents may be useful in implementing an ETSI deliverable or add to the reader's understanding, but are not required for conformance to the present document.

[i.1] ETSI GR mWT 028 (V1.1.1): "New KPI's for planning microwave and millimetre wave backhaul network".

[i.2] NGMN 0.4.2 FINAL (July 2011): "Guidelines for LTE Backhaul Traffic Estimation".

[i.3] A. K. Gupta and S. Nadarajah: "Handbook of Beta Distribution and Its Applications", Boca Raton, FL, USA: CRC Press, 2004.

[i.4] Recommendation ITU-R P.530-19 (09/2025): "Propagation data and prediction methods required for the design of terrestrial line-of-sight systems".

[i.5] Recommendation ITU-R P.676-13 (08/2022): "Attenuation by atmospheric gases and related effects".

3 Definition of terms, symbols and abbreviations

3.1 Terms

For the purposes of the present document, the following terms apply:

peak (aggregated) traffic demand: maximum value of the aggregated traffic demand process experienced by a given backhaul link

3.2 Symbols

For the purposes of the present document, the following symbols apply:

i, j, k, ℓ	generic indices
$z \in \mathcal{Z}$	z is an element of set $\mathcal{Z}$
BTA	Backhaul Traffic Availability
M	total number of capacities that can be delivered by a given backhaul link
$C_{BH}^{(i)}$	ith capacity that can be delivered by a given backhaul link (with $C_{BH}^{(1)} < C_{BH}^{(2)} < \ldots < C_{BH}^{(M)}$)
$C_{BH}^{(0)}$	link failure state
$\vartheta_{BH}^{(i)}$	availability of the ith backhaul capacity $C_{BH}^{(i)}$
$P(\mathcal{O})$	probability that event $\mathcal{O}$ occurs
T	random variable representing the aggregated traffic demand of a given backhaul link
$F_X(x)$	cumulative distribution function of a generic random variable X, evaluated at the argument x
$f_X(x, \alpha, \beta)$	probability density function of a generic Beta-distributed random variable X with parameters α and β, evaluated at the argument x
α	first shape parameter of the Beta distribution
β	second shape parameter of the Beta distribution
$\Gamma(p)$	gamma function evaluated at the argument p
$F_X(x, \alpha, \beta)$	cumulative distribution function of a generic Beta-distributed random variable X with parameters α and β, evaluated at the argument x
$I(x, \alpha, \beta)$	regularized incomplete Beta function with parameters α and β, evaluated at the argument x
$E[X]$	expected value of a generic random variable X
e^x	exponential function evaluated at the argument x
$\int_a^b g(x)dx$	integral of a generic real-valued function $g(x)$ with respect to the real variable x on an interval $[a, b]$
t_{max}	maximum (or peak) value of the generic aggregated traffic demand T
$\mathcal{M}_f$	continuous subspace of the re-scaled Beta distributions family where parameters α and β are related according to equation (10)
f	normalized average traffic demand value

N	total number of possible values for the shape parameter α in the analytical procedure for deriving BTA lower bounds
α_n	nth possible value for the shape parameter α
$\mathcal{A}$	discrete set of N possible values for the shape parameter α
β_n	nth possible value for the shape parameter β
$\mathcal{S}$	discrete set that contains all the pairs (α_n, β_n) satisfying constraint (13) on the derivative of the corresponding cumulative distribution functions
ρ	first parameter used in the analytical procedure for deriving BTA lower bounds
η	second parameter used in the analytical procedure for deriving BTA lower bounds
$\frac{\partial g(x)}{\partial x}$	derivative of a generic function $g(x)$ with respect to variable x
$g(x)\|_{x=\bar{x}}$	value of a generic function $g(x)$ evaluated at $x = \bar{x}$
γ_n	nth BTA value
$min(\mathcal{Z})$	minimum among all the real values contained in a generic discrete set $\mathcal{Z}$
$\{a_1, a_2, a_3\}$	discrete set with values a_1, a_2, a_3
$\{a_n\}_{n=1}^{N}$	discrete set with all values a_n for indices n from 1 to N
T_{max}	random variable representing the maximum values of the link input traffic observed with a given time granularity
T_{min}	random variable representing the minimum values of the link input traffic observed with a given time granularity
T_{ave}	random variable representing the average values of the link input traffic observed with a given time granularity
$F_T^{1s}(t)$	cumulative distribution function of the average link input traffic observed with a time granularity on the order of 1 second
Q	total number of bits transmitted over a backhaul link in a given time interval
S	number of seconds in a generic time interval
$E[T_{busy}]$	average throughput exchange (in bit/s) that is expected during busy hours over a given backhaul link
r_1	coefficient representing the portion of the day classified as "busy hours"
r_2	coefficient representing the anticipated traffic reduction during off-peak periods with respect to busy hours
r_3	coefficient expressing the ratio between the expected peak traffic t_{max} and the average traffic demand $E[T]$ for a given backhaul link
A_k	kth radio site of a generic backhaul network
J	total number of possible radio configurations utilized in a link planning example
$\varphi(j)$	metric value for the jth radio link configuration
$P_{Tx}^{max}(j)$	maximum transmit power (in dBm) of the radio equipment available in the jth radio link configuration
$G_{Tx}(j)$	transmit antenna gain (in dB) of the radio equipment available in the jth radio link configuration

$G_{Rx}(j)$	receive antenna gain (in dB) of the radio equipment available in the jth radio link configuration
$FM_{PIR}(j)$	PIR fade margin (in dB) guaranteed by the jth radio link configuration
$P_{Tx}^{PIR}(j)$	transmit power relative to the PIR (in dBm) of the radio equipment available in the jth radio link configuration
PL	free-space path loss (in dB) experienced over a given backhaul link
GL	attenuation due to atmospheric gases (in dB) experienced over a given backhaul link
$S_{Rx}^{PIR}(j)$	receiver sensitivity threshold relative to the PIR (in dBm) of the radio equipment available in the jth radio link configuration
$C_{BH,max}$	maximum capacity delivered by a given backhaul link
ω	coefficient expressing the ratio between the actual peak traffic value t_{max} and the maximum capacity $C_{BH,max}$ delivered by a given backhaul link
G_{tot}	overall antenna gain in dB (namely, including both the receive and the transmit side) of a given backhaul link
d	distance covered by a given backhaul link
$BTA_{\ell,d}(G_{tot})$	actual link BTA obtained for the ℓth traffic time series and the link distance d, considering an overall antenna gain equal to G_{tot}
L_i	total number of time series included in the ith test dataset
K	cardinality of the set of pairs of parameters (ρ, η) used in the numerical analysis
(ρ_k, η_k)	kth choice of a pre-defined set of K pairs of parameters (ρ, η)
$LB_{\ell,d,k}(G_{tot})$	BTA lower bound obtained for the ℓth traffic time series, the link distance d and the kth pair (ρ_k, η_k) to be used in constraint (13), considering an overall antenna gain equal to G_{tot}
$\varepsilon_{\ell,d,k}$	relative error between the BTA lower bound and the actual link BTA obtained for the ℓth time series, the link distance d and the kth pair (ρ_k, η_k) to be used in constraint (13)
$\Delta_{\ell,d,k}$	excess gain in dB needed to achieve a BTA lower bound $LB_{\ell,d,k}(G_{tot})$ numerically equal to the actual link BTA $BTA_{\ell,d}(G_{tot})$, obtained for the ℓth time series, the link distance d and the kth pair (ρ_k, η_k) to be used in constraint (13)
v_k	lower bound efficiency, defined as the percentage of cases in which the proposed analytical procedure employing the kth pair (ρ_k, η_k) in constraint (13) succeeds in generating actual BTA lower bounds
$\mathbf{1}(x)$	step function evaluated at the argument x
TCO	total cost of ownership of a target backhaul network when the traditional planning methodology is applied
I	number of resolvable intervals of the link lengths distribution of a target backhaul network
c_i	cost of the least expensive transport technology that can be employed to cover all the connection distances included in the ith interval while satisfying the target conditions of the traditional planning methodology
p_i	relative number of links in a target backhaul network with distances included in the ith interval
$TCO_{New\ KPIs}$	total cost of ownership of a target backhaul network when the New KPIs planning methodology is applied
$\tilde{c}_i$	cost of the least expensive transport technology that can be employed to cover all the connection distances included in the ith interval while satisfying the target conditions of the New KPIs planning methodology

$\mathcal{L}_n$	nth subset of links of a given backhaul network
C	generic aggregation node in a given backhaul network
ξ_k	target end-to-end BTA to be guaranteed for the traffic generated by a generic radio site A_k of a given backhaul network
$\overline{BTA}_n$	target BTA to be guaranteed over the nth link of a given backhaul network
R	number of radio sites in a generic backhaul network

3.3 Abbreviations

For the purposes of the present document, the following abbreviations apply:

2G	2nd Generation
3G	3rd Generation
4G	4th Generation
5G	5th Generation
ACM	Adaptive Coding and Modulation
ATTM	Access, Terminals, Transmission and Multiplexing
BH	Backhaul
BTA	Backhaul Traffic Availability
CDF	Cumulative Distribution Function
CIR	Committed Information Rate
DL	Downlink
ETSI	European Telecommunications Standards Institute
FDD	Frequency Division Duplex
FWA	Fixed Wireless Access
GBR	Guaranteed Bit Rate
KPI	Key Performance Indicator
LTE	Long Term Evolution
MIMO	Multiple-Input-Multiple-Output
MNO	Mobile Network Operator
mWT	millimetre Wave Transmission
PAR	Peak-to-Average Ratio
PIR	Peak Information Rate
QoE	Quality of Experience
RAN	Radio Access Network
RAT	Radio Access Technology
RTPC	Remote Transmit Power Control
SLA	Service Level Agreement
TCO	Total Cost of Ownership
TDD	Time Division Duplex
UL	Uplink

4 An analytical procedure for deriving BTA lower bounds

4.1 Overview

The aim of this clause is to present a quick and straightforward analytical procedure for deriving the lower bound of the BTA of any given backhaul link on the basis of the sole knowledge of its expected average and peak aggregated traffic demands. The proposed approach offers thus the key benefit of leading to the derivation of a worst-case (i.e. minimum achievable) BTA value that can be readily employed for a conservative and effective planning whenever an estimation of the complete statistical distribution of the expected link traffic demand is not available.

The disclosed analytical procedure builds upon the possibility to reliably capture the statistical model of the traffic demand of any transport link through a conveniently selected Beta probability distribution, as debated in [i.1]. An overview of the use of the Beta distributions family to model backhaul traffic demand dynamics is given in clause 4.2, while the method for deriving conservative BTA values is detailed in clause 4.3.

4.2 Modelling the aggregated traffic demand of backhaul links through Beta distributions

The Beta distribution is a family of parametric continuous probability distributions defined on the interval [0,1]. The analytical expressions of the probability density function

$$f_X(x,\alpha,\beta) = \frac{x^{\alpha-1}(1-x)^{\beta-1}}{\Gamma(\alpha)\Gamma(\beta)}\Gamma(\alpha+\beta), \tag{2}$$

the cumulative distribution function

$$F_X(x,\alpha,\beta) = I(x,\alpha,\beta), \tag{3}$$

and the expected value

$$E[X] = \frac{\alpha}{\alpha+\beta} \tag{4}$$

of a generic Beta-distributed random variable X depend on the value of the two positive parameters α and β, being

$$\Gamma(p) = \int_0^\infty z^{p-1}e^{-z}dz \tag{5}$$

the gamma function, and

$$I(x,\alpha,\beta) = \frac{\Gamma(\alpha+\beta)}{\Gamma(\alpha)\Gamma(\beta)} \times \int_0^x z^{\alpha-1}(1-z)^{\beta-1}dz \tag{6}$$

the regularized incomplete Beta function with parameters α and β [i.3], with $x \in [0,1]$.

Previous studies conducted by the ETSI ATTM TM_mWT community [i.1] argue that the statistical behaviour of the random variable representing the traffic demand of any backhaul link can be accurately modelled by a properly re-scaled Beta distribution. This implies that, based on relations (2), (3), and (4), the probability density function, the cumulative distribution function and the expected value of any traffic demand variable T with maximum (peak) value t_{max} can be approximated as:

$$f_T(t,\alpha,\beta) = \frac{1}{t_{max}} \times f_X\left(\frac{t}{t_{max}},\alpha,\beta\right) = \frac{t^{\alpha-1}(t_{max}-t)^{\beta-1}}{(t_{max})^{\alpha+\beta-1}\Gamma(\alpha)\Gamma(\beta)}\Gamma(\alpha+\beta), \tag{7}$$

$$F_T(t,\alpha,\beta) = I\left(\frac{t}{t_{max}},\alpha,\beta\right), \tag{8}$$

and

$$E[T] = \frac{\alpha}{\alpha+\beta}\,t_{max}, \tag{9}$$

respectively, for a convenient choice of the shape parameters α and β, and with the independent variable $t \in [0, t_{max}]$.

NOTE 1: Throughout the present document, the traffic carried over any link at any given time instant is modelled as a random variable T characterized by a statistical distribution that is assumed to remain constant over time.

NOTE 2: Terms maximum and peak are used interchangeably within the present document when referring to traffic demand random variables.

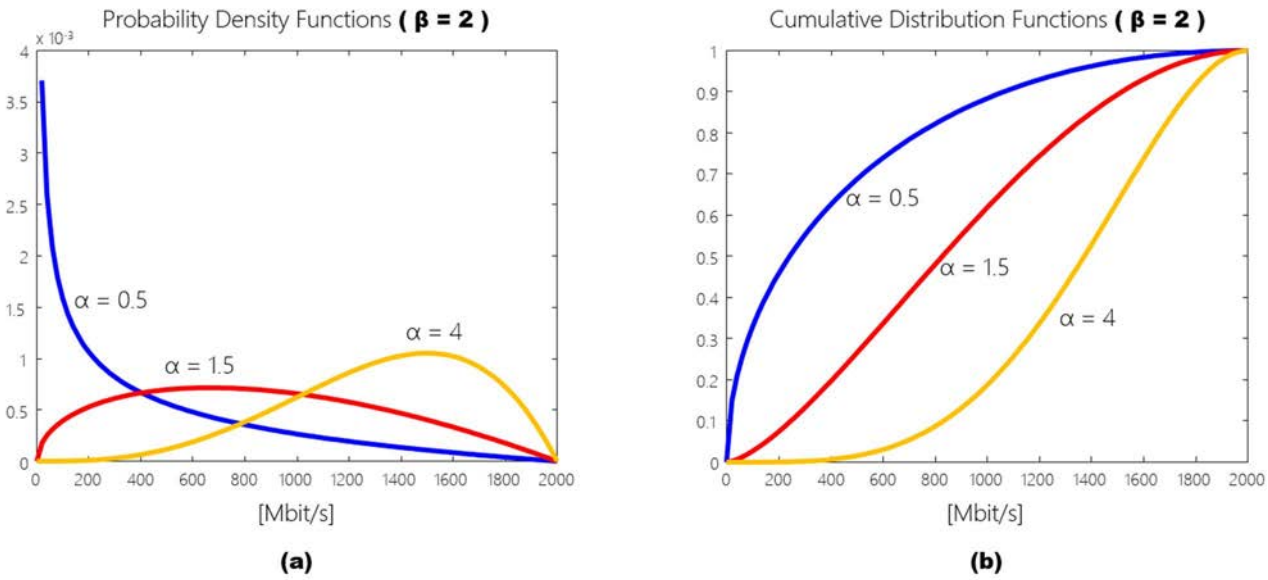

Figure 3: Illustrative probability density functions and cumulative distribution functions of Beta-distributed traffic demand random variables with fixed $\beta = 2$

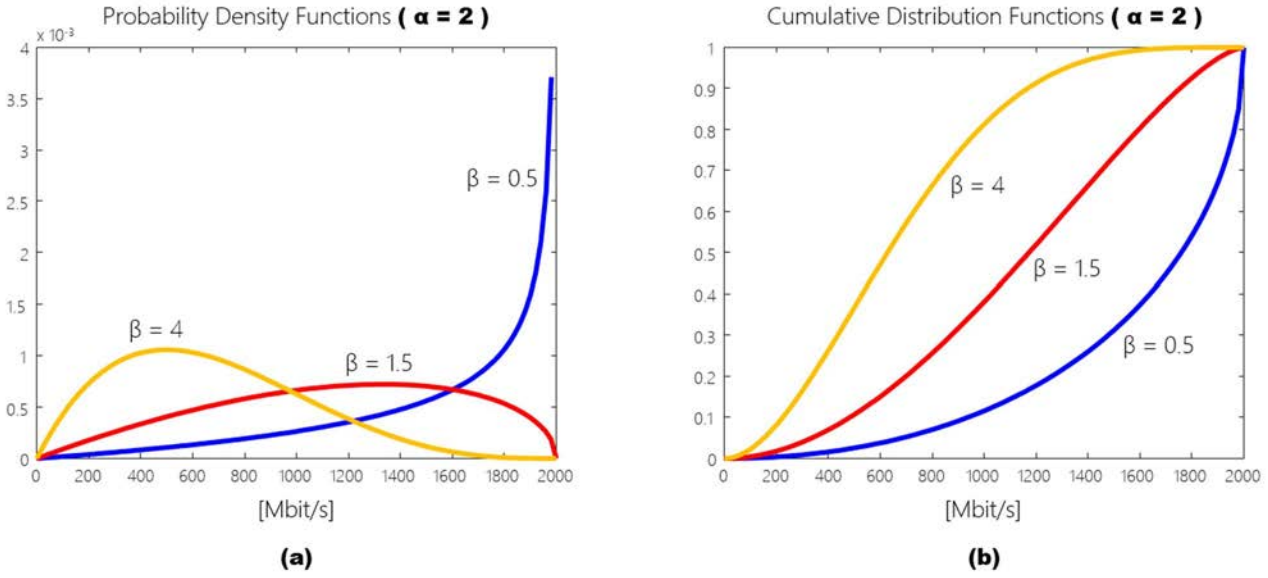

Figure 4: Illustrative probability density functions and cumulative distribution functions of Beta-distributed traffic demand random variables with fixed $\alpha = 2$

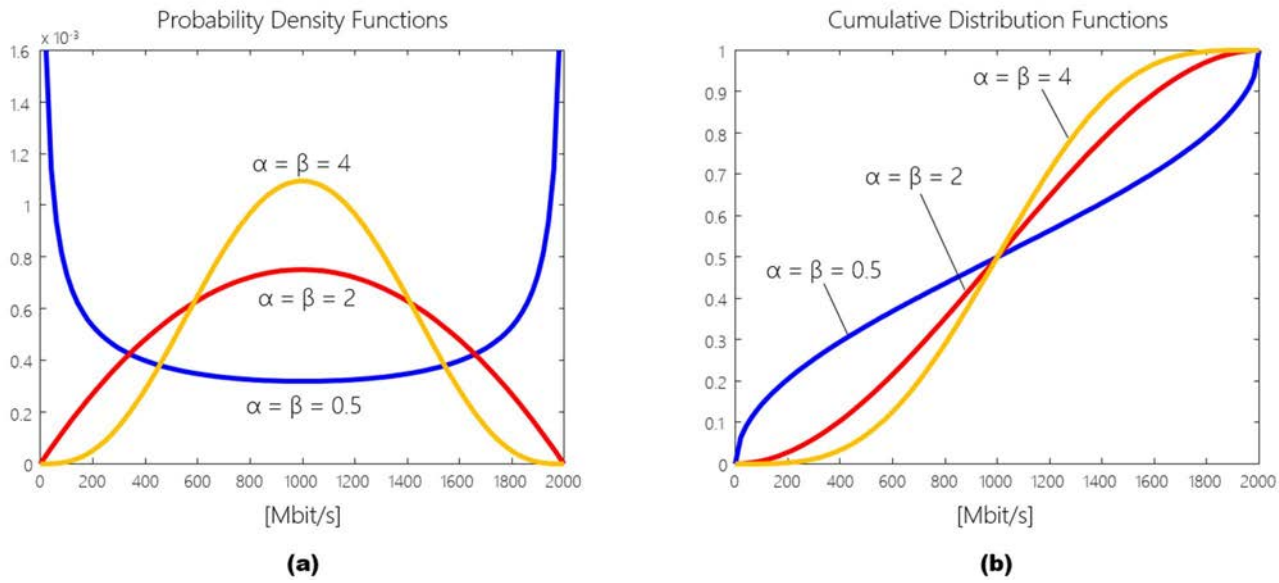

Figure 5: Illustrative probability density functions and cumulative distribution functions of Beta-distributed traffic demand random variables with $\alpha = \beta$

Figures 3, 4 and 5 show illustrative probability density functions and cumulative distribution functions of Beta-distributed traffic demand random variables with maximum value t_{max} = 2 Gbit/s, for different choices of the parameters α and β, according to equations (7) and (8). It is remarked that some combinations of α and β can lead to unrealistic traffic demand distribution shapes where high capacities tend to become more probable than values in the low-to-medium range (for example, for $\beta = 0{,}5$ in figure 4-(a) and $\alpha = \beta = 0{,}5$ in figure 5-(a)). These preliminary graphical considerations will be further expanded and elaborated in the following clause 4.3 and annex A devoted to the disclosure of the analytical procedure for deriving BTA lower bounds.

4.3 The analytical procedure for deriving BTA lower bounds

The possibility of using the Beta distributions family to approximate the statistical behaviour of any backhaul traffic demand allows to derive the analytical method disclosed in the present clause, targeted at associating any transport link with a worst-case BTA value that can be readily used for a conservative but effective planning.

According to equation (9), the ensemble of traffic demand random variables characterized by a maximum value t_{max} and an average value $E[T]$ can be statistically described by a continuous subspace $\mathcal{M}_f$ of the re-scaled Beta distributions family where parameters α and β are related according to the following rule:

$$\beta = \frac{1-f}{f}\alpha, \tag{10}$$

being

$$f = E[T]/t_{max} \tag{11}$$

the normalized average traffic demand value. By way of example, the coloured area in the chart of figure 6 illustrates the ensemble of the re-scaled Beta cumulative distribution functions belonging to the continuous subspace $\mathcal{M}_{f=0,3}$, that can be used to represent the statistical behaviour of any traffic demand random variable with normalized average value $f = E[T]/t_{max} = 0{,}3$.

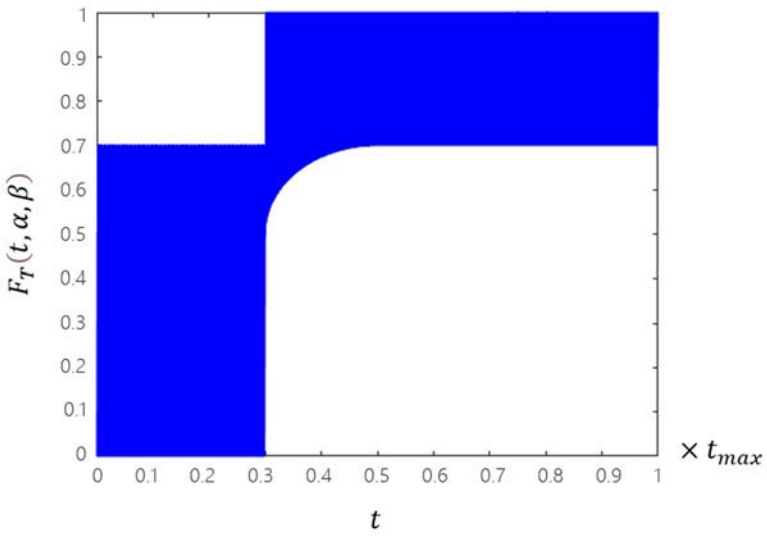

Figure 6: Ensemble of the re-scaled Beta cumulative distribution functions $F_T(t, \alpha, \beta)$ belonging to the continuous subspace $\mathcal{M}_{f=0,3}$

Once fixed the backhaul technology, which determines the ordered set of transport capacities $\left\{C_{BH}^{(i)}\right\}_{i=1}^{M}$ (with $C_{BH}^{(1)} < C_{BH}^{(2)} < \ldots < C_{BH}^{(M)}$) and the corresponding availabilities $\left\{\vartheta_{BH}^{(i)}\right\}_{i=1}^{M}$ (the latter obtainable through the application of the well-established guidelines and methods in Recommendation ITU-R P.530-19 [i.4]), the ensemble of BTA values associated with all the cumulative distribution functions belonging to the continuous subspace $\mathcal{M}_f$ lie within a closed interval for any value of the normalized average traffic demand f, as sketched in figure 7 for the illustrative case of a 3,4 km E-band backhaul connection employing 500 MHz bandwidth (therein, a peak traffic demand value t_{max} = 3 100 Mbit/s is assumed). This consideration is at the basis of the analytical procedure described in table 1, that aims, for an input pair of average and peak expected traffic demand values, at finding the BTA lower bound (i.e. the *BTA* worst-case) of any link under investigation by conducting a convenient search on the space of (α, β) parameters satisfying equation (10).

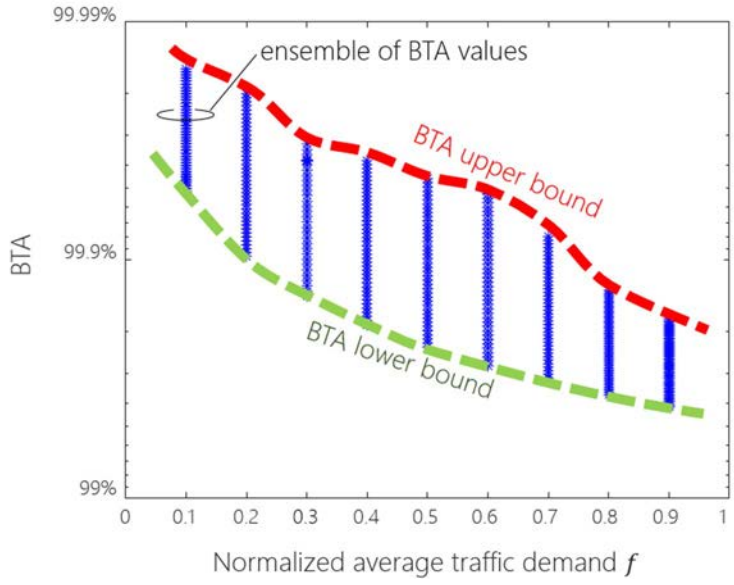

NOTE: In this figure, the set of transport capacities $\left\{C_{BH}^{(i)}\right\}_{i=1}^{M}$ and the corresponding availabilities $\left\{\vartheta_{BH}^{(i)}\right\}_{i=1}^{M}$ characterizing a 3,4 km E-band connection operating with a 500 MHz bandwidth have been utilized for deriving the ensemble of BTA values associated with all the traffic cumulative distribution functions belonging to the continuous subspaces $\mathcal{M}_f$, for different values of the normalized average demand f on the abscissa (f = 0,1, 0,2, …, 0,9), with t_{max} = 3 100 Mbit/s.

Figure 7: Ensemble of BTA values associated with all the traffic cumulative distribution functions belonging to the continuous subspaces $\mathcal{M}_f$, for different values of f

Table 1: Analytical procedure for deriving the BTA lower bound of any given backhaul link

Initialization

1) Determine the set of transport capacities $\left\{C_{BH}^{(i)}\right\}_{i=1}^{M}$ and the corresponding availabilities $\left\{\vartheta_{BH}^{(i)}\right\}_{i=1}^{M}$ of the backhaul link of interest (with $C_{BH}^{(1)} < C_{BH}^{(2)} < \ldots < C_{BH}^{(M)}$);

2) define a discrete set $\mathcal{A} = \{\alpha_n\}_{n=1}^{N}$ of N possible values for the shape parameter α, with $\alpha_n > 10^{-3}$;

3) compute the normalized average traffic demand value f according to equation (11), where:

   3a) $E[T]$ denotes the average value of the expected traffic demand over an entire year, or, if unavailable, over any time period not shorter than one full day (24 hours);

   3b) t_{max} denotes the maximum value of the expected traffic demand that can be theoretically generated by the ensemble of the RAT layers transported over the backhaul link under analysis, and it can be readily computed according to the well-established guidelines in, e.g., NGMN 0.4.2 [i.2];

4) for each value $\alpha_n \in \mathcal{A}$, compute the corresponding shape parameter β_n according to relation (10) as:

$$\beta_n = \frac{1-f}{f}\alpha_n; \tag{12}$$

5) create a discrete set $\mathcal{S}$ that contains all the pairs (α_n, β_n) satisfying the following constraint on the derivative of the corresponding cumulative distribution functions $F_T(t, \alpha_n, \beta_n)$ evaluated at $t = \rho \times t_{max}$ [bit/s]:

$$\left.\frac{\partial F_T(t,\alpha_n,\beta_n)}{\partial t}\right|_{t=\rho\times t_{max}} = f_T(t,\alpha_n,\beta_n)|_{t=\rho\times t_{max}} = \frac{1}{t_{max}} \times \frac{\rho^{\alpha_n-1}(1-\rho)^{\beta_n-1}}{\Gamma(\alpha_n)\Gamma(\beta_n)}\Gamma(\alpha_n+\beta_n) \leq \frac{\eta}{t_{max}}, \tag{13}$$

   with $\rho = 0{,}999$ and $\eta = 0{,}05$ (see annex A for a detailed explanation), and being $f_T(t, \alpha, \beta)$ the re-scaled Beta probability density function defined in equation (7);

BTA lower bound computation

6) for each pair of (α_n, β_n) parameters belonging to the set $\mathcal{S}$ derived in step 5:

   6a) compute the probabilities that the link traffic demand T falls in the adjacent intervals $\left[C_{BH}^{(i-1)}, C_{BH}^{(i)}\right]$ $(i = 1,2, \ldots, M)$ as:

$$P\left(C_{BH}^{(i-1)} < T \leq C_{BH}^{(i)}\right) = F_T\left(C_{BH}^{(i)}, \alpha_n, \beta_n\right) - F_T\left(C_{BH}^{(i-1)}, \alpha_n, \beta_n\right), \tag{14}$$

   being $C_{BH}^{(0)} = 0$ bit/s the link failure state, and

$$F_T(t, \alpha_n, \beta_n) = I\left(\frac{t}{t_{max}}, \alpha_n, \beta_n\right) \tag{15}$$

   the re-scaled Beta cumulative distribution function with shape parameters (α_n, β_n), according to equation (8);

   6b) estimate the corresponding BTA value γ_n according to equation (1);

7) return $min(\{\gamma_n\}_{n=1}^{N})$ as the **worst-case BTA value** (i.e. the **BTA lower bound**) for the link under consideration.

It is remarked that, while steps 1 through 4 lead to the creation of a discretized version of the continuous subspace $\mathcal{M}_f$ (for the selected value of f), the additional constraint (13) has the role of further limiting the search space over the two parameters (α, β) in order to improve the tightness of the lower bound with respect to the distribution of all the possible BTAs that can realistically occur in practical scenarios. More specifically, inequality (13), imposing that the derivative of the cumulative distribution functions $F_T(t, \alpha_n, \beta_n)$ evaluated at $\rho \times t_{max}$ is lower than $0{,}05/t_{max}$ (with $\rho = 0{,}999$), sets a restriction on the maximum slope of the admissible CDFs in the high-traffic region (see figure 8 for a graphical explanation). This leads to the final effect of including in the search process of the BTA lower bounds only the shape parameters (α_n, β_n) associated with distributions where high traffic demands occur with progressively smaller probabilities with respect to lower capacities, thus excluding, by way of example, the unrealistic behaviours previously outlined in figures 4 and 5 (i.e. for $\beta = 0{,}5$ in figure 4-(a) and $\alpha = \beta = 0{,}5$ in figure 5-(a)). For illustration, the ensemble of the re-scaled Beta cumulative distribution functions $F_T(t, \alpha, \beta)$ corresponding to traffic demand random variables with normalized average value $f = E[T]/t_{max} = 0{,}3$ that satisfy inequality (13) is plotted in figure 9.

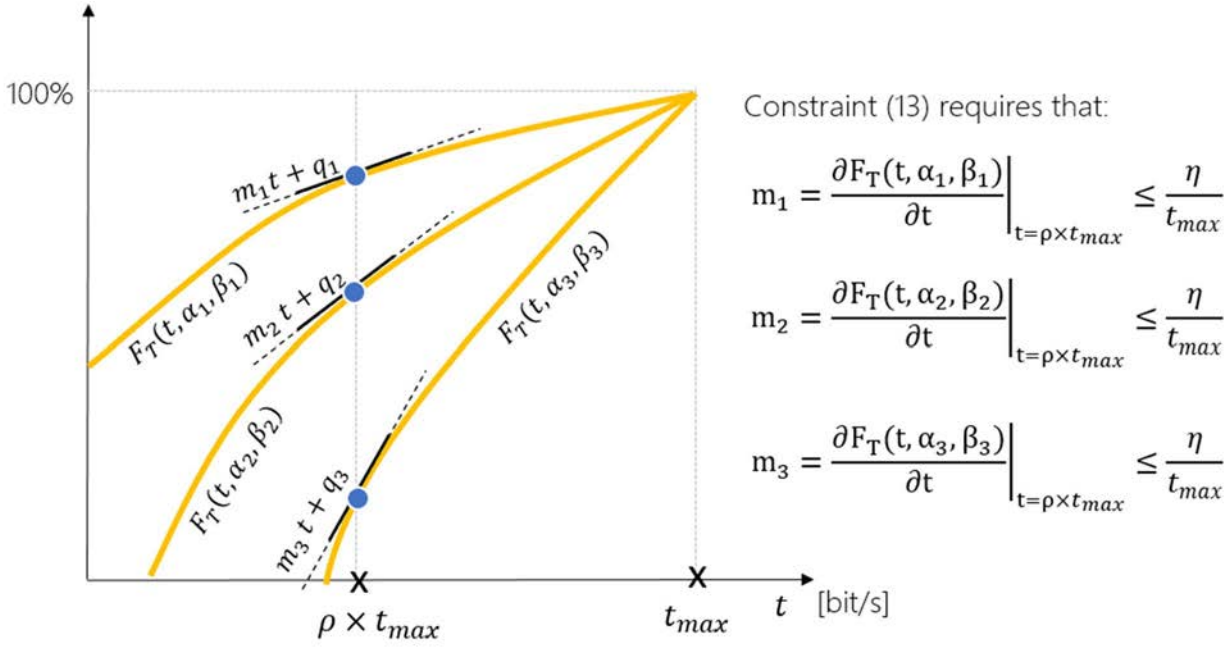

NOTE: This figure shows that, according to constraint (13), the local slopes m_1, m_2 and m_3 of the cumulative distribution functions $F_T(t, \alpha_1, \beta_1)$, $F_T(t, \alpha_2, \beta_2)$ and $F_T(t, \alpha_3, \beta_3)$ of illustrative traffic demand random variables, respectively, evaluated at $t = \rho \times t_{max}$ should be $\leq \eta/t_{max}$.

Figure 8: A graphical representation of constraint (13)

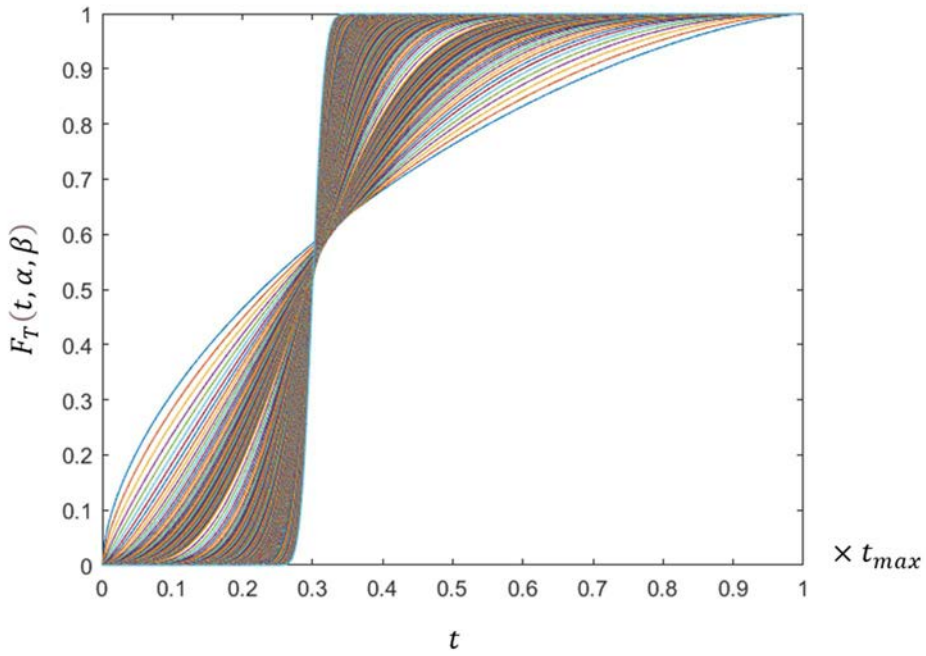

Figure 9: Ensemble of the re-scaled Beta cumulative distribution functions $F_T(t, \alpha, \beta)$ corresponding to traffic demand random variables with normalized average value $f = E[T]/t_{max} = 0,3$ that satisfy inequality (13)

The analytical expression of constraint (13), along with the choice for parameters ρ and η, has been defined on the basis of the results of an extensive simulation campaign conducted on a database of realistic traffic time series collected from live backhaul networks (see annex A for a detailed description of the employed methodology).

The computational complexity of the whole analytical procedure illustrated in table 1 scales linearly with the cardinality N of the initial set $\mathcal{A}$ of parameters α. The totality of the numerical results and evaluations based on the dataset of traffic time series described in annex A suggests that values of N on the order of a few hundred are sufficient to optimize the intrinsic trade-off between lower bound accuracy and computational complexity of the proposed method. Consequently, the disclosed procedure is expected to be easily integrable into currently commercialized software planning tools with minimal resource demands.

5 Traffic demand distribution models through measurement campaigns on live networks

5.1 Overview

The definition of appropriate prediction models of the backhaul traffic demand statistics can lead to the strategic benefit of making the choice of the throughput distributions required for computing the BTA metric a process completely transparent to the end user, and can thus greatly contribute to the successful adoption of the New KPIs methodology. In this context, the availability of realistic measurements collected from operative networks is recognized as crucial to enable the definition first and the validation then of effective traffic distribution forecast strategies.

The present clause 5 is devoted to the presentation of a methodology for conducting measurement campaigns on live transport networks with the ultimate goals of:

1) obtaining a proprietary database of cumulative distribution functions of the traffic demand experienced by a statistically relevant set of backhaul links deployed in different environmental (e.g. in terms of topology and subscribers' density) and technological (e.g. in terms of transported RAN configurations) conditions;

2) grouping the obtained traffic demand distributions into homogeneous clusters of links with similar features;

3) describing each cluster of links through a compact set of representative CDFs of the traffic demand (e.g. in terms of the 5th percentile lower-bound, the 95th percentile upper-bound and the median cumulative distribution functions as better explained in the following) to be subsequently used as references in the planning phase of any network according to the New KPIs methodology.

General guidelines for the collection, classification and clustering of traffic data will be provided in clauses 5.2, 5.3, and 5.4, respectively, while a discussion on the experimental results obtained during the preparation of the present document will be matter of clause 5.5.

5.2 Data collection

To assess the novel BTA metric (defined in equation (1)), ETSI GR mWT 028 [i.1] recommends to employ the cumulative distribution function of the average input traffic demand of the link observed with a time granularity on the order of 1 second. The present clause is devoted to discuss practical guidelines to achieve an estimate of this latter link feature by solely relying on the performance monitoring systems already available in the currently deployed wireless transport networks.

As a first observation, it is remarked that the input traffic demand of a given backhaul link - theoretically definable as the amount of pure end-to-end throughput unaffected by any bottleneck possibly introduced by the link itself - represents a quantity that is inherently difficult - if not impossible - to measure directly. As a practical and reasonable approximation, the input traffic demand can be assumed to correspond to the input traffic of the backhaul link under consideration measured at the ingress port (see figure 10 for a schematic representation), provided that the link operates under (virtually) ideal propagation and deployment conditions to avoid any possible capacity reductions or congestion effects (such as those caused by fading-related outages).

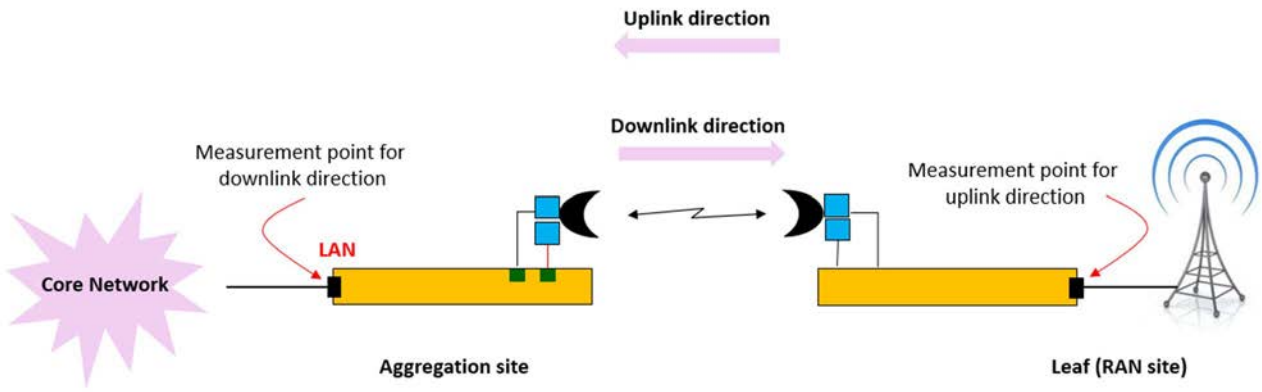

Figure 10: Recommended measurement points for the input traffic flowing over the backhaul link under consideration in both the downlink and the uplink directions

Secondly, performance monitoring systems implemented in currently deployed backhaul networks typically provide aggregated measurements of the input traffic of each link (such as the maximum, the minimum and the average values) with a time granularity on the order of minutes (e.g. 15 minutes), which makes the collection of raw throughput data with higher sampling rates (e.g. with a temporal resolution on the order of 1 second as specified in ETSI GR mWT 028 [i.1]) not achievable. It is further observed that, although monitoring systems are continuously evolving and will soon enable the measurement of per-link input traffic dynamics at time granularities as fine as one second, opting for coarser resolutions will always remain a viable choice - particularly in contexts where minimizing the signalling overhead constitutes a priority.

Based on these practical considerations, effective measurement campaigns should be aimed at inspecting a statistically relevant number of wireless transport links and at obtaining, for each of them:

- a cumulative distribution function $F_{T_{max}}(t)$ of the random variable T_{max} representing the maximum values of the input traffic observed with the lowest possible time granularity (usually on the order of minutes in current networks), being t the independent variable expressed in bit/s;
- a cumulative distribution function $F_{T_{min}}(t)$ of the random variable T_{min} representing the minimum values of the input traffic observed with the lowest possible time granularity;

- a cumulative distribution function $F_{T_{ave}}(t)$ of the random variable T_{ave} representing the average values of the input traffic observed with the lowest possible time granularity.

Since, though, input traffic values are typically sampled at the transmit devices with intrinsic integration times (and, therefore, granularities) of few seconds - before being aggregated into wider time periods for the use of current performance monitoring systems -, it is here emphasized that, for any backhaul link, the cumulative distribution function $F_T^{1s}(t)$ of the average input traffic observed with a time granularity on the order of 1 second as specified in ETSI GR mWT 028 [i.1]:

i) is upper-bounded and lower-bounded by $F_{T_{min}}(t)$ and $F_{T_{max}}(t)$, respectively; and

ii) is quite accurately represented by $F_{T_{ave}}(t)$ in the median region, as sketched in figure 11.

Therefore, computing the BTA of any link through equation (1) by employing cumulative distribution function $F_{T_{max}}(t)$ will always produce a more pessimistic value compared to the one based on $F_T^{1s}(t)$.

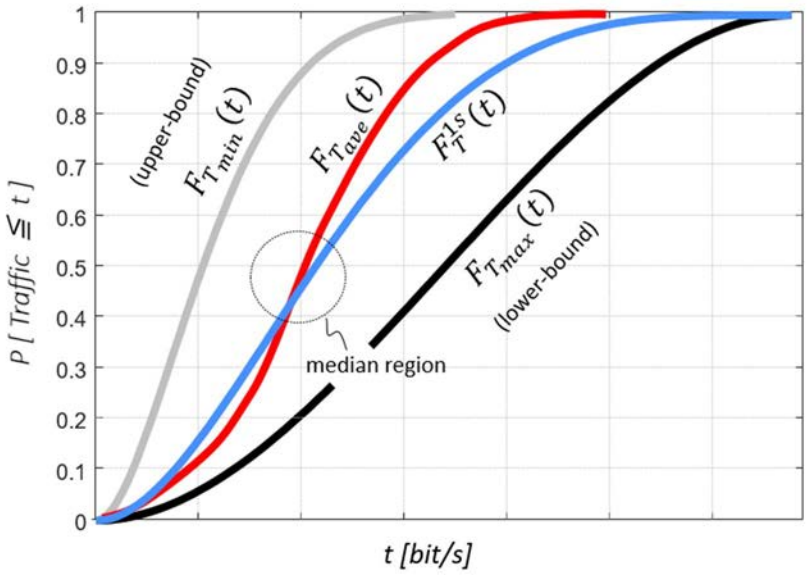

Figure 11: Schematic representation of the cumulative distribution functions $F_{T_{max}}(t)$, $F_{T_{min}}(t)$, $F_{T_{ave}}(t)$ and $F_T^{1s}(t)$

Tighter approximations to the actual cumulative distribution function $F_T^{1s}(t)$ of the average input traffic observed with a time granularity on the order of 1 second could be achieved by linearly combining the aggregated throughput measurements T_{max}, T_{min} and T_{ave} with coarser resolutions, or the corresponding functions $F_{T_{max}}(t)$, $F_{T_{min}}(t)$ and $F_{T_{ave}}(t)$ defined before. Activities aimed at defining the preferred methodology for this purpose should rely on validations using traffic data sampled at intervals on the order of a few seconds as ground truth.

A step in this direction has been made during the preparation of the present document by recording for 1 week the traffic dynamics - with a time granularity of 1 second - of two tail links (namely, providing backhaul connectivity to single multi-band LTE RAN sites) and two feeder links (aggregating three and four LTE RAN sites respectively) deployed in both urban and rural areas of an EU Country. Afterwards, the derived datasets have been processed in order to derive, for each link:

- the cumulative distribution function $F_T^{1s}(t)$ of the originally measured traffic time series with 1 second time granularity;
- the cumulative distribution functions $F_{T_{max}}(t)$, $F_{T_{min}}(t)$ and $F_{T_{ave}}(t)$ of the random variables T_{max}, T_{min} and T_{ave} representing the maximum, minimum and average traffic values over adjacent 15-minute time windows, respectively;
- the cumulative distribution function obtained by averaging $F_{T_{max}}(t)$ and $F_{T_{min}}(t)$;
- the cumulative distribution function of the random variable $(T_{max} + T_{min})/2$.

The test outcomes are summarized in figure 12, illustrating that, in all cases, the CDF of the random variable $(T_{max} + T_{min})/2$ provides the closest approximation to the target function $F_T^{1s}(t)$. Consequently, this CDF should also be considered as a relevant output of the data collection phase for each link. Specifically, the results of the experimental activity described in clause 5.5 will be entirely based on this latter statistical distribution.

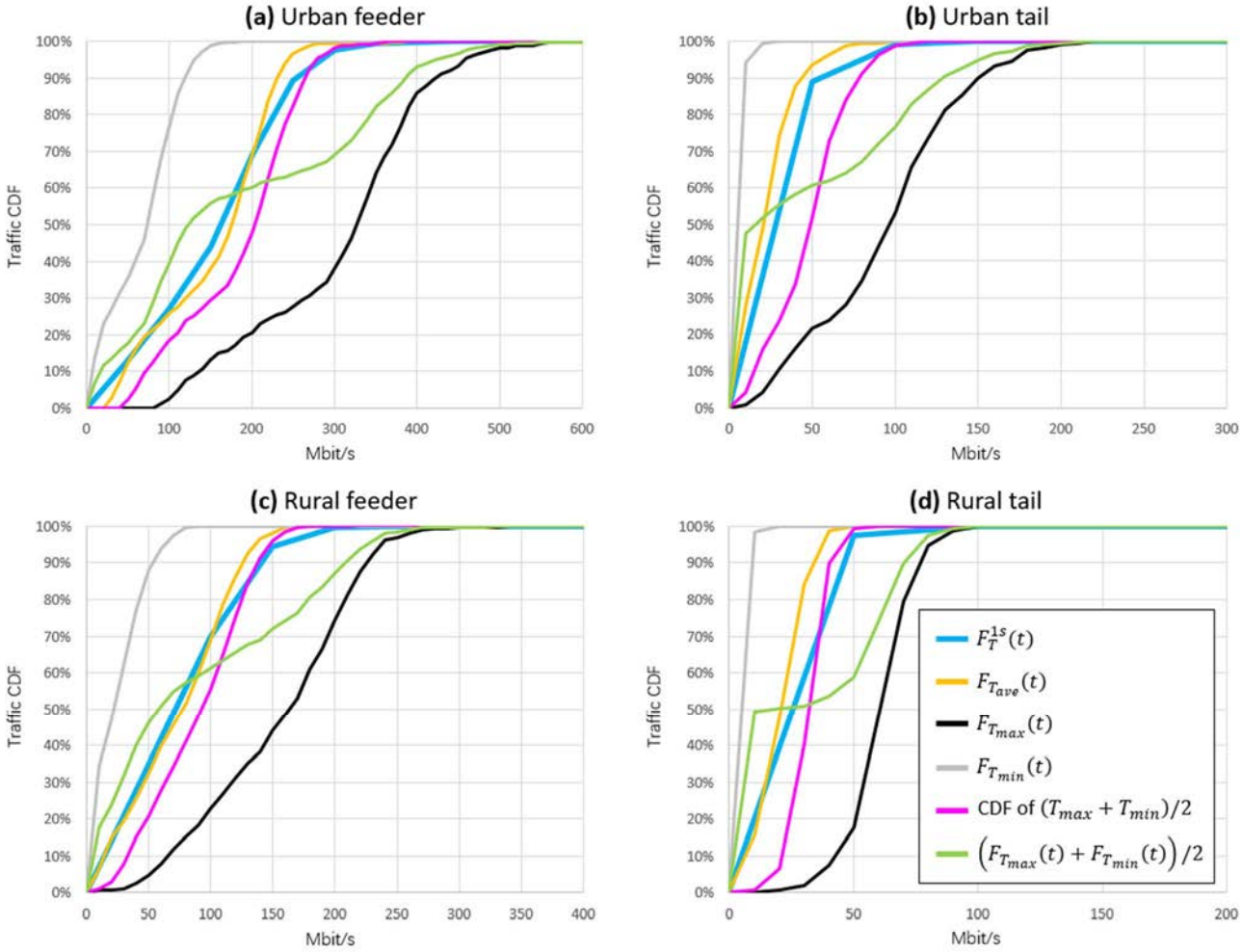

Figure 12: Cumulative distribution functions $F_T^{1s}(t)$ of the average input traffic measured with a time granularity on the order of 1 second compared with the cumulative distribution functions obtained on the basis of throughput data aggregated over adjacent 15-minute time windows

5.3 Data classification

Each traffic cumulative distribution function obtained by applying the guidelines described in clause 5.2 should be also associated with a list of significant attributes (also referred to as labels in the following) characterizing the link under analysis, e.g. including the deployment conditions and the involved RAN technologies and configurations.

The factors with the highest impact on the traffic statistical behaviour and that should be primarily considered in the link classification process are expected to belong to the following macro-categories:

1) Location of the transported RAN sites.

2) Type of the transported RATs.

3) Number of radio layers for each transported RAT.

4) Number of cells per site, utilized bandwidth, duplex mode and MIMO configuration for each transported radio layer.

Further details and insights about these attributes are discussed in the following.

1) Location of the transported RAN sites

RAN sites with the same technological configurations can generate different amounts of traffic, depending on the deployment area and the users' distribution. Moreover, a precise classification of the site location can provide important indications about the future RAN traffic growth, that in turn can be used in the elaboration of accurate throughput demand prediction models.

Sites deployed in urban or dense-urban areas are characterized by higher loads than rural locations and could be of stronger interest for mobile operators as they can generate more revenues.

2) Type of the transported RATs

The data streams flowing over the currently deployed backhaul links typically originate from a mix of 2G, 3G, 4G, and 5G RATs. However, since 4G and 5G layers are generally the primary contributors to the overall exchanged throughput, focusing exclusively on these latter technologies can greatly streamline the classification process without, on the other hand, compromising the validity of the analysis. Accordingly, the focus should be restricted to identify only the following possible categories:

- 4G-only sites, with or without Fixed Wireless Access (FWA) users
- 5G-only (stand-alone) sites, with or without FWA users
- Dual 4G/5G sites, with or without FWA users

The FWA attribute is currently seen by the industry as a crucial traffic booster in 5G deployments, and it is therefore expected to play a key role in the determination of the traffic patterns.

3) Number of radio layers for each transported RAT

Even within the same geographical region, different RAN sites can vary significantly in the number and configuration of 4G and 5G technologies. LTE sites deployed in urban or dense-urban areas are typically equipped with:

- an underlying layer ensuring coverage, usually operating in the lowest available frequency bands (700 MHz, 800 MHz, or 900 MHz), with a bandwidth of 10 MHz or 15 MHz (most commonly 10 MHz) and utilizing 2x2 MIMO base stations;
- one or two additional layers in higher frequency bands (1 800 MHz, 2 100 MHz, 2 300 MHz, or 2 600 MHz), designed to boost capacity in densely populated areas. These layers usually operate with a bandwidth of 20 MHz or multiples thereof and rely on 4x4 MIMO base stations.

The same pattern of coverage and additional high-capacity layers is also expected for mature 5G installations. Table 2 complements this description by providing an example of different RAN site configurations (from column six to eight) deployed in the same urban area of an existing 4G and 5G mobile network.

Table 2: Example of different RAN site configurations (from column six to eight) deployed in the same urban area of an existing 4G and 5G mobile network

RAN technology	Bandwidth [MHz]	Duplex Technology	MIMO	Number of cells	Configuration 1	Configuration 2	Configuration 3
4G 800 MHz	10	FDD	2x2	3	x	x	x
4G 1 800 MHz	20	FDD	2x2	3		x	
4G 2 100 MHz	15	FDD	2x2	3		x	
4G 1 800 MHz	20	FDD	4x4	3	x		
4G 2 100 MHz	15	FDD	4x4	3	x		
5G 2 600 MHz	90	TDD	4x4	3		x	
5G 3 500 MHz	100	TDD	4x4	3	x	x	

4) Number of cells per site, utilized bandwidth, duplex mode and MIMO configuration for each transported radio layer

Each radio access technology layer can provide connectivity to various cells per site (typically three or four in urban or dense-urban scenarios, but even up to six in specific cases), with different duplex modes (e.g. TDD or FDD) and MIMO configurations (2x2 or 4x4 MIMO for 4G, and massive MIMO for 5G), leading to an enormous number of possible combinations. To simplify the overall data collection and classification process, measurement campaigns should focus on the most probable configurations, and proper scaling laws could be defined in order to predict the relevant statistical properties of traffic in less frequent scenarios.

Based on the most relevant macro-categories described above, a reference list of labels that could be used for classifying the measured backhaul links is provided in table 3, that also includes implementation-oriented indications that can foster future software integration. Additionally, the illustrative values reported in the last column have been derived by considering an exemplary backhaul link aggregating traffic from two radio sites deployed in a densely populated and non-touristic urban area:

- the first site is configured with two 4G layers (with 10 MHz and 15 MHz bandwidth, respectively), both carrying mobile-only traffic via 2x2 MIMO FDD base stations, and one 5G layer (100 MHz bandwidth), also carrying mobile-only traffic via 64x64 massive MIMO TDD base stations with a DL:UL ratio of 80:20;
- the second site hosts three 4G layers with 20 MHz, 15 MHz and 20 MHz bandwidth, respectively, all carrying both mobile and FWA traffic through 4x4 MIMO FDD base stations.

In the considered example, all RATs have been assumed to operate with three sectors.

Table 3: Reference list of labels for traffic data classification

Type	No.	Label	Values	Unit	Example
Site	1	N Aggregated Sites	Integer (1 in case of Tail link, >1 in case of Feeder link)		2
	2	Coverage Type	list of letters ∈ [**D** (Dense-Urban), **U** (Urban), **S** (Sub-Urban), **R** (Rural)] with length "N Aggregated Sites"		D D
	3	Area Type	list of letters ∈ [**T** (Touristic), **N** (Non Touristic)] with length "N Aggregated Sites"		N N
4G	4	**4G** RAT Layers	list of integers with length "N Aggregated Sites"		2 3
	5	**4G** Bandwidth	list of integers with length "sum(**4G** RAT Layers)"	[MHz]	10, 15 20, 15, 20
	6	**4G** MIMO Layers Tx	list of integers with length "sum(**4G** RAT Layers)"		2, 2 4, 4, 4
	7	**4G** MIMO Layers Rx	list of integers with length "sum(**4G** RAT Layers)"		2, 2 4, 4, 4
	8	**4G** Duplex Mode	list of strings ∈ [**FDD** (for FDD), **TDD_90**, **TDD_80**, **TDD_70**, **...**, **TDD_10** (for TDD with DL:UL ratio equal to 90:10, 80:20, 70:30, ..., 10:90, respectively)] with length "sum(**4G** RAT Layers)"		FDD, FDD FDD, FDD, FDD
	9	**4G** Sectors	list of integers with length "sum(**4G** RAT Layers)"		3, 3 3, 3, 3
	10	**4G** Service Type	list of strings ∈ [**NN**, **NY**, **YN**, **YY**] with length "sum(**4G** RAT Layers)" **(see note below)**		NN, NN YN, YN, YN
5G	11	5G RAT Layers	list of integers with length "N Aggregated Sites"		1 0
	12	**5G** Bandwidth	list of integers with length "sum(**5G** RAT Layers)"	[MHz]	100
	13	**5G** MIMO Layers Tx	list of integers with length "sum(**5G** RAT Layers)"		64
	14	**5G** MIMO Layers Rx	list of integers with length "sum(**5G** RAT Layers)"		64
	15	**5G** Duplex Mode	list of strings ∈ [**FDD** (for FDD), **TDD_90**, **TDD_80**, **TDD_70**, **...**, **TDD_10** (for TDD with DL:UL ratio equal to 90:10, 80:20, 70:30, ..., 10:90, respectively)] with length "sum(**5G** RAT Layers)"		TDD_80
	16	**5G** Sectors	list of integers with length "sum(**5G** RAT Layers)"		3
	17	**5G** Service Type	list of strings ∈ [**NN**, **NY**, **YN**, **YY**] with length "sum(**5G** RAT Layers)" **(see note below)**		NN

Type	No.	Label	Values	Unit	Example
NOTE:	First letter in each string of labels 10 and 17 in table 3 is **Y** (=Yes) if site carries FWA traffic, while it is **N** (=No) otherwise; second letter is **Y** (=Yes) if site carries Enterprise traffic, while it is **N** (=No) otherwise. Mobile traffic is assumed present by default.				

5.4 Clustering of traffic demand distributions

The ensemble of measured and properly classified traffic CDFs should be then assigned to a reduced set of homogeneous clusters on the basis of their respective link attributes. Afterwards, a group of representative cumulative distribution functions should be identified for each cluster, such as (see figure 13 for reference):

- the median CDF, the 95th percentile upper-bound CDF (excluding 5 % of CDFs with higher values), and the 5th percentile lower-bound CDF (excluding 5 % of CDFs with lower values) of the cluster of cumulative distribution functions $F_{T_{max}}(t)$ of the random variables T_{max} representing the maximum values of the link input traffic observed with the lowest possible time granularity (e.g. 15 minutes);
- the median CDF, the 95th percentile upper-bound CDF, and the 5th percentile lower-bound CDF of the cluster of cumulative distribution functions of the random variables $(T_{max} + T_{min})/2$, where T_{max} and T_{min} represent the maximum and minimum traffic values, respectively, of the link input traffic observed with the lowest possible time granularity (e.g. 15 minutes).

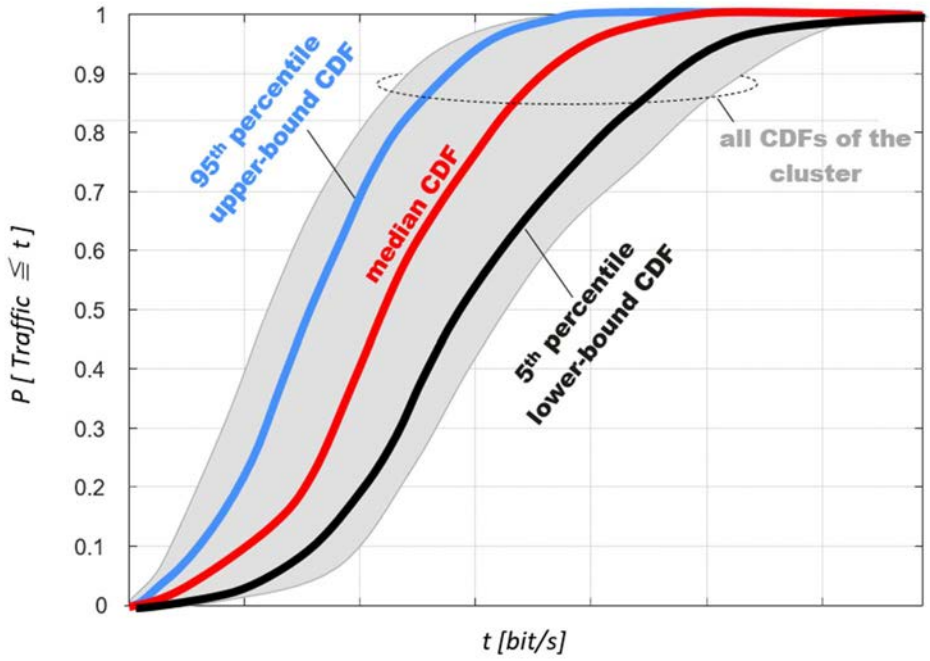

Figure 13: Schematic representation of the median CDF, the 95th percentile upper-bound CDF and the 5th percentile lower-bound CDF of a given cluster of cumulative distribution functions

Any subsequent planning process according to the New KPIs methodology should be then built upon:

i) the association of the link under analysis with one of the derived clusters (on the basis of its attributes); and

ii) the assessment of the BTA through equation (1) by using one of the six representative CDFs mentioned above.

A recommended strategy is to base the link design on the choice of the 5th percentile lower-bound CDF of the random variables $(T_{max} + T_{min})/2$ as a mildly conservative scenario. Alternatively, the 5th percentile lower-bound CDF of the random variables T_{max} can be adopted in case a more precautionary approach is preferred.

In addition, each cluster of CDFs may be further processed to derive reference average and maximum traffic values to be used as inputs for the application of the analytical procedure for deriving BTA lower bounds as described in clause 4.3.

5.5 Experimental results

The present clause 5.5 illustrates the results of a measurement campaign conducted with the primary goal of providing a guideline on how to apply the methodologies described in clauses 5.2 through 5.4, which are targeted to identify the representative traffic statistical distributions of a set of reference RAN scenarios to be directly utilized in the BTA assessment.

For this purpose, a total of 535 wireless backhaul links deployed in rural and sub-urban areas of a European Country have been monitored for the entire month of January 2024. All links provide connectivity to single three-sector RAN sites equipped with 4G (in all cases) and possibly 5G technology (in nearly 50 % of cases). As for the 4G layer, the communication in each sector is ensured by 2x2 MIMO base stations employing a total bandwidth ranging from 10 MHz to 80 MHz across several combinations of one-to-six frequency bands, all operated in FDD mode. When present, the 5G layer is implemented in the C-Band and utilizes base stations equipped with 64 transmit and 64 receive antennas. An indication on whether the different sites are deployed in touristic areas and deliver FWA services is also available (see table 4 and table 5 for more detailed statistics on the investigated links).

Table 4: Distribution of the total 4G bandwidth utilized by the RAN sites reached by the backhaul links under analysis

	Total RAN sites	RAN sites equipped with 5G	RAN sites in touristic areas	RAN sites providing FWA services
10 MHz	12	0	0	0
15 MHz	4	0	0	0
20 MHz	6	0	2	0
25 MHz	79	20	5	17
30 MHz	32	10	4	10
35 MHz	18	3	2	2
40 MHz	1	0	0	0
45 MHz	190	89	24	82
50 MHz	3	0	2	0
60 MHz	161	108	36	97
80 MHz	29	16	9	17
Total	**535**	**246**	**84**	**225**

Table 5: Correlation among RAN sites equipped with 5G technology, sites deployed in touristic areas and sites providing FWA services

	5G	Touristic	FWA
5G	**246**	27	223
Touristic	27	**84**	23
FWA	223	23	**225**

During the experimental campaign, the bidirectional time series of the maximum, average and minimum percent bandwidth utilization within the one-month observation period have been extracted and recorded for each link with a time granularity of 15 minutes by leveraging the available performance monitoring systems. Then, the measured bandwidth utilization time series have been converted into traffic time series - in bit/s - by considering the actual interface port speed of the link equipment in each 15-minute time window. For every link, only the communication direction with the highest transported capacities (carrying downlink radio access flows) has been accounted for in the analysis presented in this clause.

Afterwards, the selected traffic time series of each link have been used to derive the relevant CDFs as detailed in clause 5.2, which in turn have been accurately classified by applying the guidelines in clause 5.3. The successive clustering phase has been based on the only cumulative distribution functions of the random variables $(T_{max} + T_{min})/2$ of each link, obtained by averaging the minimum and the maximum throughput values measured at 15-minute intervals, as the best approximation to the CDFs of the traffic observed with a time granularity on the order of 1 second recommended for computing the BTA according to ETSI GR mWT 028 [i.1] (see clause 5.2). Furthermore, the analysis has been restricted to the three largest 4G bandwidth categories identified in table 4 - namely 25 MHz, 45 MHz, and 60 MHz - thereby narrowing the considered dataset to a subset of 430 links out of the original 535.

Grouping the selected traffic time series on the basis of the total amount of 4G bandwidth leads to the three clusters of cumulative distribution functions illustrated in figures 14-(a), 14-(b) and 14-(c), where only the median CDF, the 95th percentile upper-bound CDF and the 5th percentile lower-bound CDF are drawn for each case, according to the guidelines in clause 5.4. Despite the fact that there are significant differences in the statistical behaviour of the traffic produced by the three bandwidths - as outlined by figure 14-(d) that summarizes the 50th percentile and the 99th percentile values of the median CDF of each group -, the resulting three clusters of cumulative distribution functions mostly overlap (as shown in figure 15, where all lines in figures 14-(a), 14-(b) and 14-(c) are superimposed in the same plot).

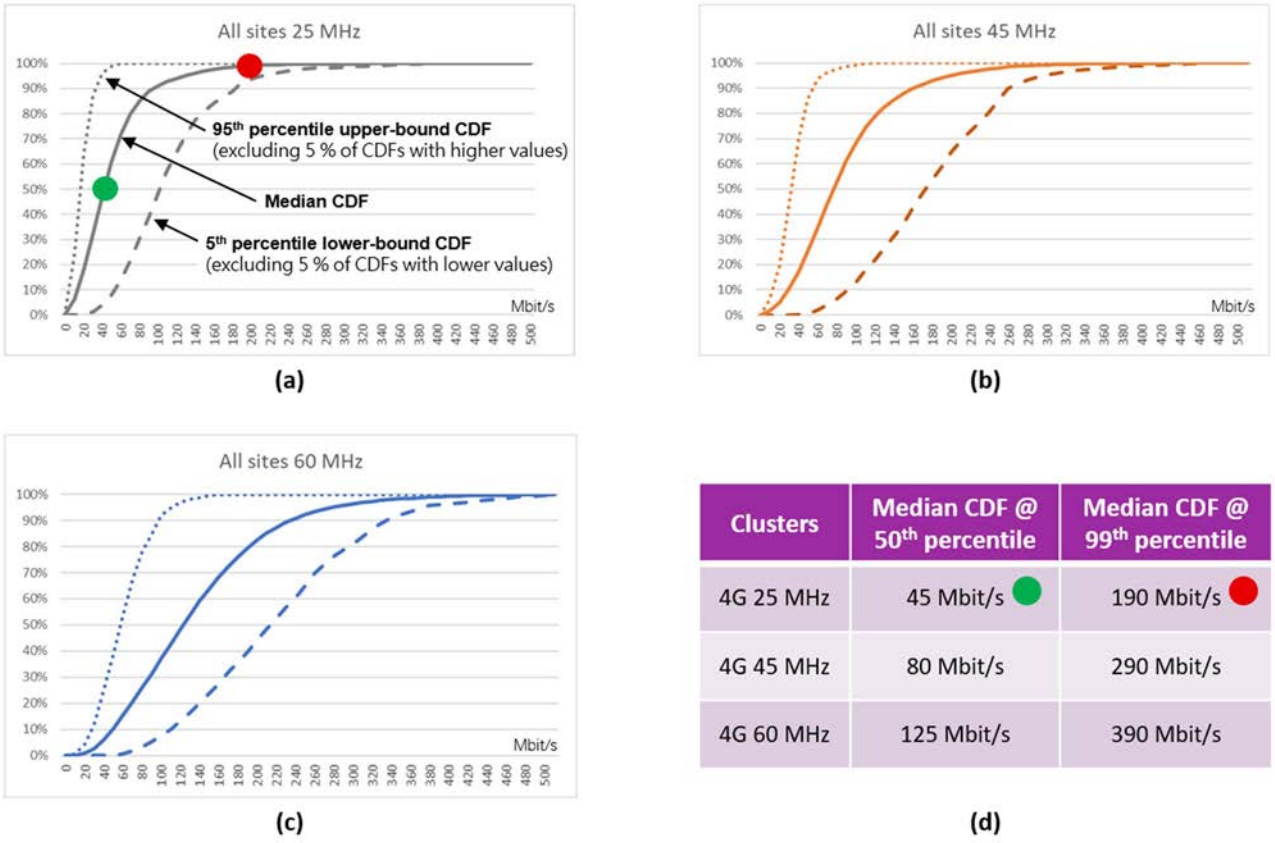

Clusters	Median CDF @ 50th percentile	Median CDF @ 99th percentile
4G 25 MHz	45 Mbit/s	190 Mbit/s
4G 45 MHz	80 Mbit/s	290 Mbit/s
4G 60 MHz	125 Mbit/s	390 Mbit/s

Figure 14: Representative CDFs and reference values of the three clusters of cumulative distribution functions derived by employing the only total 4G bandwidth information

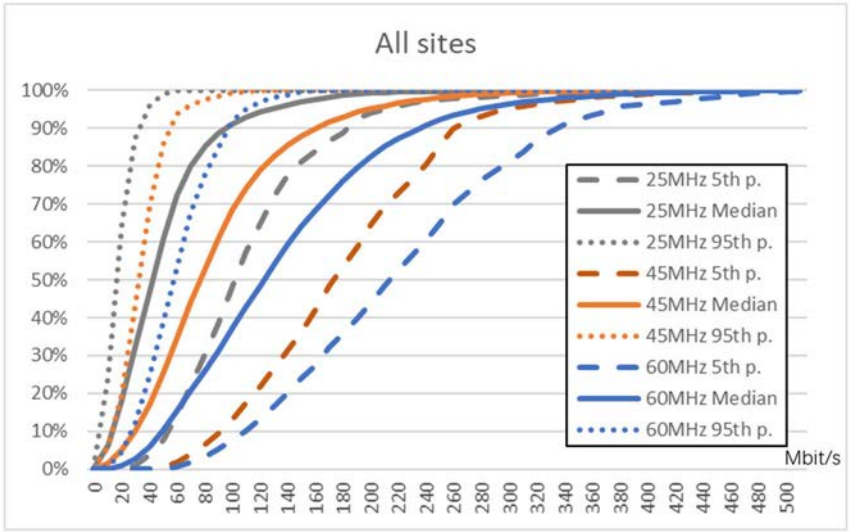

Figure 15: Superposition of the median CDF, the 95th percentile upper-bound CDF and the 5th percentile lower-bound CDF of each of the three clusters in figure 14

A further level of grouping of the traffic time series based on a second attribute becomes therefore necessary to obtain more distinguishable clusters with a reduced spread between the 95th percentile upper-bound and the 5th percentile lower-bound CDFs. Among all the available link information, the "Touristic" label has not been considered due to both the limited number of surveyed sites with this feature and the observation period (falling in the off-peak season), while both the 5G and FWA attributes have been investigated separately (although almost all 5G sites also provide FWA services, as reported in table 5) obtaining, e.g., figure 16 for the case of 25 MHz total 4G bandwidth (similar outcomes have been achieved for 45 MHz and 60 MHz). The plots suggest that a further grouping of the traffic time series either on the basis of the presence or absence of 5G technologies in the connected sites (figure 16-(a)), or on the basis of the presence or absence of FWA services (figure 16-(b)), represents an effective strategy for decreasing the spread of the identified clusters, thus confirming, as expected, the key role of the 5G and FWA dimensions in the clustering process. Unfortunately, the strong correlation among sites equipped with 5G radio access technology and those offering FWA services does not allow to appreciate the mutually exclusive use of these two important labels. Therefore, the second clustering dimension of the present study can only be formulated as "links carrying 5G and/or FWA traffic".

The considerations expressed in the present clause, even if related to a limited number of surveyed links, provide a first example of how to apply the methodology described in clauses 5.2 through 5.4, and corroborate the importance of some of the key clustering attributes identified in clause 5.3.

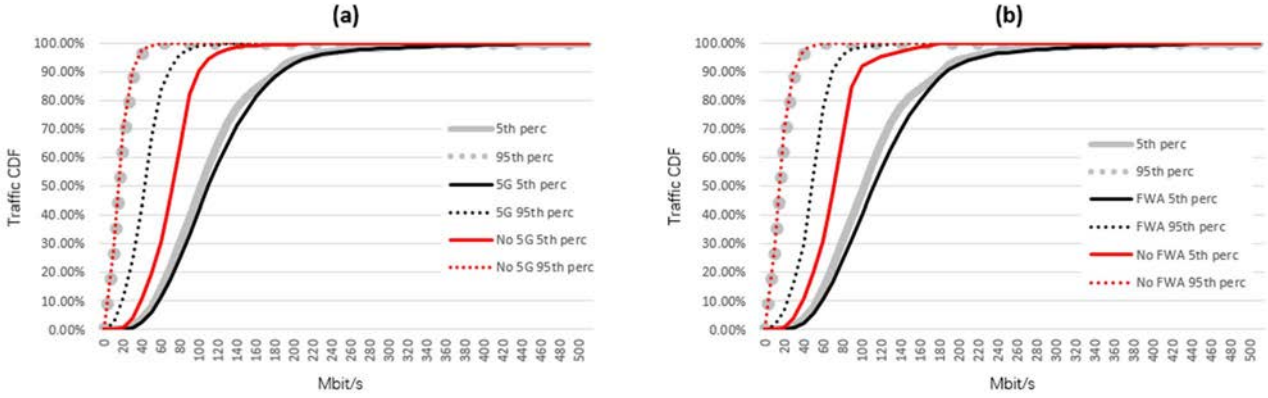

NOTE: This figure shows the 95th percentile upper-bound CDFs and 5th percentile lower-bound CDFs of the clusters of traffic time series with or without 5G data streams (in black and red colour, respectively, in (a)), and with or without FWA services (in black and red colour, respectively, in (b)) for the only case of 25 MHz total 4G bandwidth. As a reference, the lower-bound and upper-bound CDFs of the overall cluster with a total of 25 MHz 4G bandwidth (i.e. considering the first classification attribute only) are also shown in both (a) and (b) in grey.

Figure 16: Clusters of traffic time series with or without 5G data streams and with or without FWA services for the case of 25 MHz total 4G bandwidth

6 Link planning example

6.1 Overview

The present clause 6 is entirely devoted to the description of a comprehensive planning procedure based on the New KPIs methodology, with specific reference to the illustrative backhaul scenario sketched in figure 17. Before delving into the link design example, clause 6.2 explores practical strategies for determining both the average and the peak values of the expected traffic demand of any backhaul link of interest, that are key parameters for the application of the analytical procedure for deriving BTA lower bounds, as outlined in clause 4. Afterwards, clause 6.3 gets to the heart of the case study by describing the main system and link assumptions, followed by clauses 6.4 and 6.5 which illustrate the planning workflow by applying the methods for computing the BTA metric detailed in the previous parts of the present document.

6.2 Derivation of the average and the peak values of the expected link traffic demand

As highlighted in clause 4, the analytical procedure for deriving BTA lower bounds relies on the availability of accurate estimates of both the **average traffic demand** $E[T]$ and the **peak traffic demand** t_{max} expected over the transport link under consideration. Specifically:

- $E[T]$ denotes the average value of the expected traffic demand over an entire year, or, if unavailable, over any period not shorter than one full day (24 hours);
- t_{max} denotes the maximum value of the expected traffic demand that can be theoretically generated by the ensemble of the transported RAT layers.

While well-defined guidelines exist for computing the peak throughput values (e.g. as outlined in NGMN 0.4.2 [i.2] and illustrated in figure 1 for the illustrative case of a RAN site with three sectors), there is currently no standardized approach for estimating the average traffic demands. In practice, the derivation of the latter quantities is often carried out using proprietary tools developed by mobile network operators or vendors, whose internal mechanisms and specifications fall outside the scope of the present document. Nevertheless, to ensure a self-contained and accessible methodology, a few approaches that have been recognized as valid during the preparation of the present document are outlined below. Alternative strategies - either derived from those listed here or complementary to them - may also be adopted.

1) Determination from empirical measurements

The average traffic demand value $E[T]$ (in bit/s) for the link of interest can be estimated by measuring the total number of bits Q transmitted over a transport connection with similar characteristics (e.g. in terms of the attributes illustrated in clause 5) during a time interval of S seconds (with $S \geq 86\,400$), and then dividing the observed quantity by S, as:

$$E[T] = \frac{Q}{S} \quad \left[\frac{bit}{s}\right] \tag{16}$$

2) Determination from busy hours average traffic

The average traffic demand value $E[T]$ (in bit/s) for the link of interest can be estimated by appropriately scaling the average throughput exchange $E[T_{busy}]$ (in bit/s) that is expected during busy hours according to the following expression:

$$E[T] = E\left[T_{busy}\right]r_1 + E\left[T_{busy}\right]r_2(1 - r_1) \quad \left[\frac{bit}{s}\right], \tag{17}$$

where coefficient r_1 (≤ 1) represents the portion of the day classified as "busy hours", and r_2 (≤ 1) reflects the anticipated traffic reduction during off-peak periods.

EXAMPLE: Assuming 8 hours of busy time per day and a 50 % reduction of the average traffic during off-peak hours with respect to $E\left[T_{busy}\right]$, it would yield $r_1 = 8/24 = 1/3$ and $r_2 = 1/2$.

In this case, the average traffic value $E[T_{busy}]$ during busy hours can be obtained either through simulation or by direct measurement of transport connections that exhibit similar characteristics (e.g. in terms of the attributes described in clause 5) to the link of interest.

NOTE: Throughout the present document, the expression busy hours denotes the specific time period during the day when a network or system experiences its highest volume of activity or traffic.

3) Determination from the peak traffic value

The average traffic demand value $E[T]$ (in bit/s) for the link of interest can be estimated as a fraction of the expected peak traffic t_{max} (in bit/s) as:

$$E[T] = \frac{t_{max}}{r_3} \left[\frac{bit}{s}\right], \tag{18}$$

where the scaling factor r_3 can be chosen in the range $[3,8]$ when the target backhaul link connects a single RAN site. For a conservative network planning, a value of $r_3 = 3$ should be selected.

6.3 Scenario description

Clause 6 pursues the task of planning a bidirectional backhaul connection between two radio sites at a distance of 5,3 km and deployed in a geographical region where rainfall intensities exceed 32 mm/h for 0,01 % of the time in a year (see figure 17 for reference). The expected traffic volume to be transported across the two communication paths is unbalanced, and it is characterized by a peak load t_{max} = 3,5 Gbit/s and an average value $E[T]$ = 1,36 Gbit/s in the direction with the highest demand - both of which are known parameters.

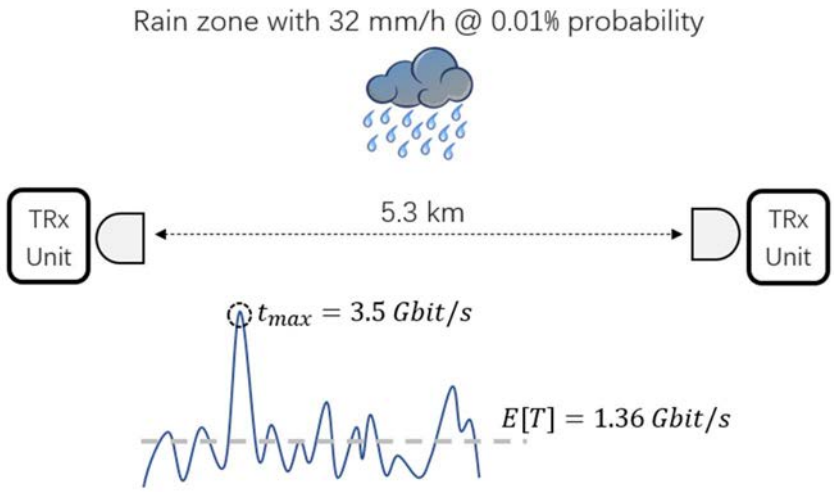

Figure 17: Overview of the illustrative backhaul scenario considered in clause 6, with information on the link distance, the rain zone and the main traffic statistical parameters

Based on this objective, the selected radio equipment consists of a single-polarization transceiver unit operating in the E-band, featuring a bandwidth of 500 MHz and a maximum output power of 26 dBm, with a maximum gross information rate equal to 4,5 Gbit/s yielding a net throughput greater than the expected peak traffic load t_{max}. The unit supports an Adaptive Coding and Modulation (ACM) policy, and it is therefore capable of dynamically adjusting the delivered capacities according to the fading conditions along the propagation path.

In this scenario, two types of parabolic antennas are assumed to be available: one with a diameter of 30 cm (maximum gain of 45,4 dBi), and another with a diameter of 60 cm (maximum gain of 51,4 dBi). These give rise to three possible radio link configurations:

- **Configuration 1**: one E-band unit equipped with 30 cm antenna at both the radio sites;
- **Configuration 2**: one E-band unit with 30 cm antenna at the first site and one E-band unit with 60 cm antenna at the second site;
- **Configuration 3**: one E-band unit with 60 cm antenna at both the radio sites.

The purpose of clause 6 is to define the optimal radio link configuration to ensure compliance with the following target conditions, derived from a New-KPIs-oriented link planning methodology (see Introduction for further details):

- CIR = 25 Mbit/s available for at least 99,995 % of the time

- BTA higher than 99,97 %
- Gross PIR = 4,5 Gbit/s with at least 5 dB of fade margin

It is observed that the BTA constraint expressed above can be interpreted, for instance, as stemming from the application of the apportionment rule outlined in annex A of the ETSI GR mWT 028 [i.1] to the network topology depicted in figure 18, where three radio sites - A_1, A_2 and A_3 - are connected to a remote aggregation node C in a daisy-chain configuration (see annex C for further details on the recommended guidelines for BTA apportionment in generalized network scenarios). Specifically, the selection of the target BTA values for each link illustrated in the diagram ensures that the traffic generated by each of the three radio sites achieves an overall end-to-end BTA (i.e. up to node C) that consistently meets or exceeds the threshold of 99,9 % recommended in [i.1].

Figure 18: Illustrative BTA apportionment for a network topology with three radio sites connected to a remote aggregation point in a daisy-chain configuration

Two distinct link planning procedures are outlined in the following, depending on whether an estimate of the complete statistical distribution of the expected traffic demand, in addition to the provided peak and average values (t_{max} and $E[T]$, respectively), is available or not.

6.4 Link planning with known traffic distribution

When an estimate of the cumulative distribution function $F_T(t)$ of the link's target traffic demand is available - such as from the employment of the measurement-based methodology described in clause 5 - the planning procedure should follow the general steps specified in table 6.

Table 6: Link planning procedure according to the New KPIs methodology with known cumulative distribution function of the link's target traffic demand

Initialization

1) For each jth radio link configuration, compute the following metric:

$$\varphi(j) = P_{Tx}^{max}(j) + G_{Tx}(j) + G_{Rx}(j) \quad (19)$$

as the sum of the maximum transmit power $P_{Tx}^{max}(j)$ (in dBm), the transmit antenna gain $G_{Tx}(j)$ (in dB) and the receive antenna gain $G_{Rx}(j)$ (in dB) of the available radio equipment;

2) sort the available radio link configurations in ascending order based on the metric $\varphi(j)$, to obtain:

$$\varphi(1) < \varphi(2) < \cdots < \varphi(J), \quad (20)$$

being J the total number of radio link configurations;

3) initialize $j = 1$;

Link Planning

4) compute the metrics prescribed by the New KPIs methodology considering the jth radio link configuration:

4a) derive the PIR fade margin $FM_{PIR}(j)$ as:

$$FM_{PIR}(j) = P_{Tx}^{PIR}(j) + G_{Tx}(j) + G_{Rx}(j) - PL - GL - S_{Rx}^{PIR}(j), \quad (21)$$

where $P_{Tx}^{PIR}(j)$ is the transmit power of the radio equipment relative to the PIR (in dBm), $G_{Tx}(j)$ an $G_{Rx}(j)$ are defined as in step 1, PL is the free-space path loss (in dB), GL is the attenuation due to atmospheric gases (in dB), and $S_{Rx}^{PIR}(j)$ is the receiver sensitivity threshold relative to the PIR (in dBm);

NOTE: Term GL can be computed according to Recommendation ITU-R P.676-13 [i.5].

4b) derive the availability $\vartheta_{BH}^{(i)}(j)$ of each ith backhaul capacity $C_{BH}^{(i)}$ (with $C_{BH}^{(1)} < C_{BH}^{(2)} < \ldots < C_{BH}^{(M)}$) according to the well-established methodologies based on the fading prediction models described in Recommendation ITU-R P.530-19 [i.4];

4c) for all indexes $i = 1,2, \ldots, M$, compute the probability $P\left(C_{BH}^{(i-1)} < T \leq C_{BH}^{(i)}\right)$ that the link throughput demand lies in the range between backhaul capacities $C_{BH}^{(i-1)}$ and $C_{BH}^{(i)}$ on the basis of the target traffic cumulative distribution function $F_T(t)$ (assumed known in the present clause) as:

$$P\left(C_{BH}^{(i-1)} < T \leq C_{BH}^{(i)}\right) = F_T\left(C_{BH}^{(i)}\right) - F_T(C_{BH}^{(i-1)}), \quad (22)$$

being $C_{BH}^{(0)} = 0$ bit/s the link failure state;

4d) derive the BTA γ_j through the formula presented in equation (1), which is reported here for ease of reference and improved readability:

$$\gamma_j = \sum_{i=1}^{M} P(C_{BH}^{(i-1)} < T \leq C_{BH}^{(i)}) \times \vartheta_{BH}^{(i)}(j), \quad (23)$$

where terms $\vartheta_{BH}^{(i)}(j)$ and $P(C_{BH}^{(i-1)} < T \leq C_{BH}^{(i)})$ (for $i = 1,2, \ldots M$) have been obtained in previous steps 4b and 4c, respectively;

5) if the PIR fade margin $FM_{PIR}(j)$, the BTA γ_j and the CIR availability derived in step 4 meet the planning targets, then end the procedure and plan the link with the jth radio configuration, otherwise increment the counter j by 1;

6) if $j \leq J$ repeat the process starting from step 4, otherwise end the procedure and conclude that no radio link configuration among the available ones can meet the planning targets.

NOTE: The initialization phase presented in table 6 (and in following table 8) serves solely as an illustrative example. Its purpose is to organize the candidate radio link configurations in a logical sequence, in order to begin with the simplest (i.e. least costly) option and to progressively test more complex (or expensive) solutions in the subsequent Link Planning steps 4, 5 and 6, until all New KPIs target conditions are satisfied. Depending on the specific context, alternative and more sophisticated sorting criteria can be necessary to accommodate varying strategic needs.

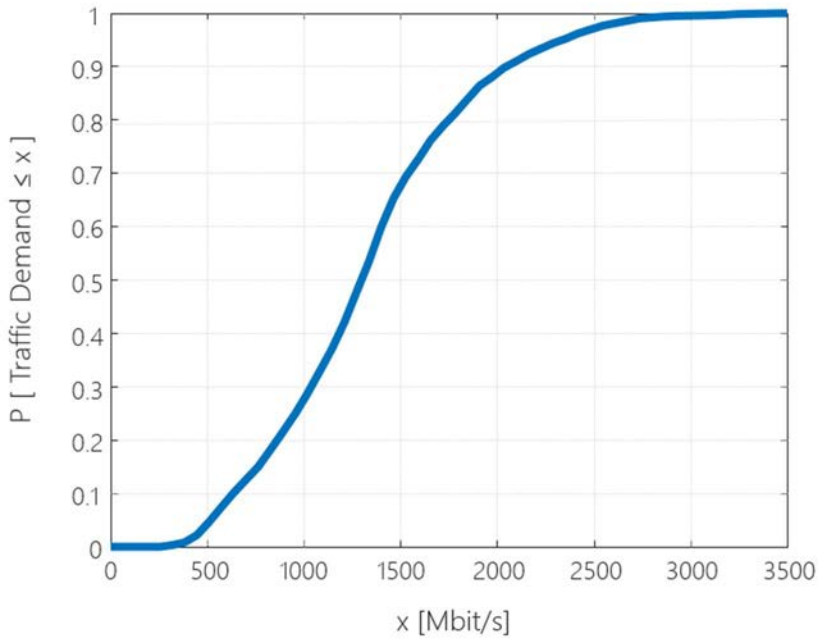

Figure 19: Cumulative distribution function $F_T(t)$ of the link's target traffic demand used to derive the BTA values in table 7 through equations (22) and (23)

Table 7 shows the values of the PIR fade margin $FM_{PIR}(j)$, the BTA γ_j and the CIR availability that can be obtained by applying steps 4a through 4d of the methodology in table 6 to each jth radio link configuration defined in clause 6.3 (here $j = 1,2,3$), assuming that the cumulative distribution function $F_T(t)$ of the link's target traffic demand is the one depicted in figure 19. Based on the reported outcomes, it can be easily deduced that the planning procedure of table 6 would result in the selection of the second radio link configuration ($j = 2$), that delivers the minimum system gain needed to satisfy all the New KPIs target conditions specified in clause 6.3.

To provide a broader perspective, the results presented in table 7 are complemented by the plot in figure 20, that illustrates the variation of:

i) the PIR fade margin (right y-axis);

ii) the BTA calculated according to equation (23) on the basis of the link's target traffic demand distribution shown in figure 19 (left y-axis);

iii) the lower bound of the BTA derived through the analytical procedure described in clause 4.3 (which forms the core of the approach discussed in the following clause 6.5) (left y-axis); and

iv) the CIR availability (left y-axis)

as a function of the combined transmission and reception antenna gains. As a reference, the gain levels ensured by radio link configurations 1, 2 and 3, corresponding to 90,8 dBi, 96,8 dBi and 102,8 dBi, respectively, are also highlighted on the x-axis.

Table 7: Key results obtained by applying steps 4a through 4d of the planning procedure illustrated in table 6 to the radio link configurations described in clause 6.3

Radio link configuration	PIR fade margin $FM_{PIR}(j)$	BTA γ_j	CIR availability
$j = 1$	9,26 dB	99,964 %	99,995 %
$j = 2$	15,28 dB	99,978 %	99,997 %
$j = 3$	21,30 dB	99,986 %	99,998 %

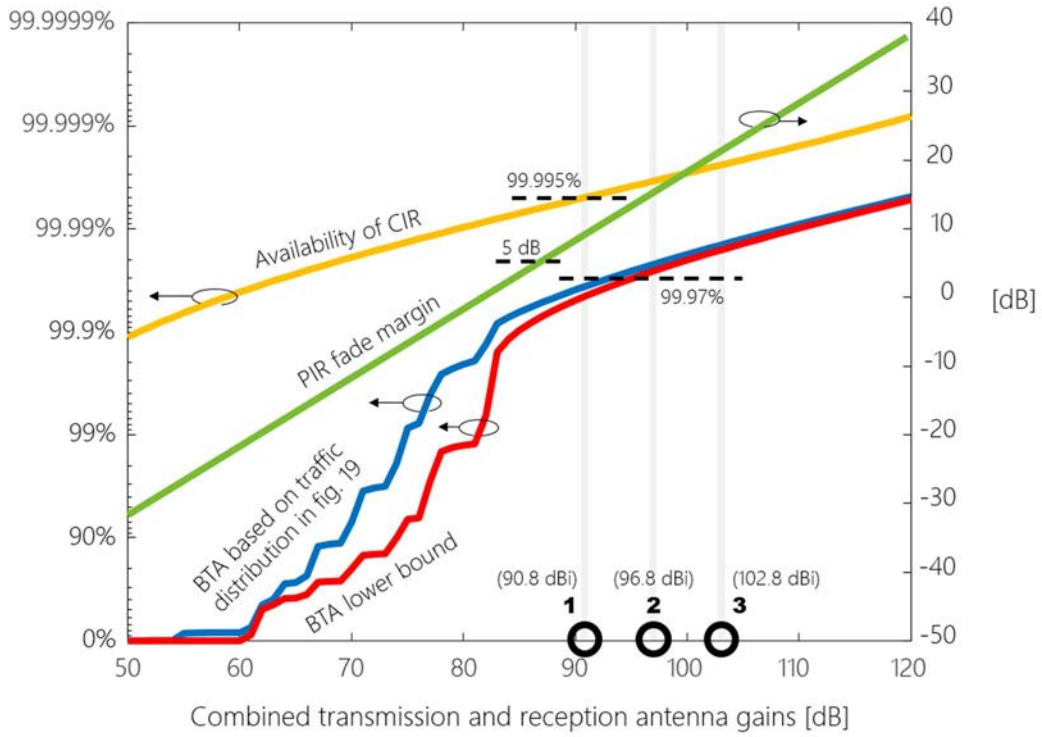

Figure 20: Variation of the metrics used in the New KPIs planning methodology as a function of the combined transmission and reception antenna gains

It is remarked that, while the example discussed in the present clause 6 involves selecting only the size of the antennas to complete the link design process, other planning scenarios could be more complex and involve candidate radio configurations with also variations in the total output powers provided at the antenna port, arising, for instance, from the availability of different product versions or the implementation of Remote Transmit Power Control (RTPC) policies - which ultimately result in limitations on the effective radiated power and are thus sensitive to the employed transmission antenna gains. Nevertheless, the approach outlined in table 6 can be easily extended to account for these additional cases.

6.5 Link planning with unknown traffic distribution

When the information on the link's target traffic demand distribution is not available, the BTA computation should be based on the conservative but effective approach described in clause 4.3. Table 8 illustrates all the steps needed to plan any backhaul link according to the New KPIs methodology in this case.

Table 8: Link planning procedure according to the New KPIs methodology with unknown cumulative distribution function of the link's target traffic demand

Initialization

1) For each jth radio link configuration, compute the following metric:

$$\varphi(j) = P_{Tx}^{max}(j) + G_{Tx}(j) + G_{Rx}(j) \quad (24)$$

as the sum of the maximum transmit power $P_{Tx}^{max}(j)$ (in dBm), the transmit antenna gain $G_{Tx}(j)$ (in dB) and the receive antenna gain $G_{Rx}(j)$ (in dB) of the available radio equipment;

2) sort the available radio link configurations in ascending order based on the metric $\varphi(j)$, to obtain:

$$\varphi(1) < \varphi(2) < \cdots < \varphi(J), \quad (25)$$

being J the total number of radio link configurations;

3) initialize $j = 1$;

Link Planning

4) compute the metrics prescribed by the New KPIs methodology considering the *j*th radio link configuration:

4a) derive the PIR fade margin $FM_{PIR}(j)$ as:

$$FM_{PIR}(j) = P_{Tx}^{PIR}(j) + G_{Tx}(j) + G_{Rx}(j) - PL - GL - S_{Rx}^{PIR}(j), \quad (26)$$

where $P_{Tx}^{PIR}(j)$ is the transmit power of the radio equipment relative to the PIR (in dBm), $G_{Tx}(j)$ an $G_{Rx}(j)$ are defined as in step 1, PL is the free-space path loss (in dB), GL is the attenuation due to atmospheric gases (in dB), and $S_{Rx}^{PIR}(j)$ is the receiver sensitivity threshold relative to the PIR (in dBm);

NOTE: Term GL can be computed according to Recommendation ITU-R P.676-13 [i.5].

4b) derive the availability $\vartheta_{BH}^{(i)}(j)$ of each *i*th backhaul capacity $C_{BH}^{(i)}$ (with $C_{BH}^{(1)} < C_{BH}^{(2)} < \ldots < C_{BH}^{(M)}$) according to the well-established methodologies in Recommendation ITU-R P.530-19 [i.4];

4c) derive the BTA lower bound by following the analytical procedure detailed in clause 4.3 (table 1), using as inputs the current availabilities $\left\{\vartheta_{BH}^{(i)}(j)\right\}_{i=1}^{M}$ (computed in step 4b) and the average and the peak values of the expected traffic demand $E[T]$ and t_{max}, respectively;

5) if the PIR fade margin $FM_{PIR}(j)$, the BTA lower bound and the CIR availability derived in step 4 meet the planning targets, then end the procedure and plan the link with the *j*th radio configuration, otherwise increment the counter *j* by 1;

6) If $j \leq J$ repeat the process starting from step 4, otherwise end the procedure and conclude that no radio link configuration among the available ones can meet the planning targets.

Table 9 reports the values of the PIR fade margin $FM_{PIR}(j)$, the BTA lower bound and the CIR availability that can be derived by applying steps 4a through 4c of the methodology in table 8 to each *j*th radio link configuration. Comparing these results with the New KPIs target conditions specified in clause 6.3 clearly indicates that, also in this case, the overall planning procedure in table 8 would designate configuration 2 as the preferred radio technology for the link under study.

Table 9: Key results obtained by applying steps 4a through 4c of the planning procedure illustrated in table 8 to the radio configurations described in clause 6.3

Radio link configuration	PIR fade margin $FM_{PIR}(j)$	BTA lower bound	CIR availability
$j = 1$	9,26 dB	99,955 %	99,995 %
$j = 2$	15,28 dB	99,974 %	99,997 %
$j = 3$	21,30 dB	99,984 %	99,998 %

For the sake of clearness, the results obtained from the application of the analytical method of clause 4.3 are here reported for the only case of configuration 1 (first row of table 9). Specifically, table 10 shows the set $\mathcal{A}$ of the test parameters $\{\alpha_n\}_{n=1}^{N}$ selected in the present example (as per step 2 of the procedure in table 1), the corresponding $\{\beta_n\}_{n=1}^{N}$ parameters derived from equation (12), the indication on whether constraint (13) is satisfied or not, and the resulting BTAs $\{\gamma_n\}_{n=1}^{N}$. In the examined scenario, the analytical method would yield a BTA lower bound equal to 99,955 %, which corresponds to the minimum value among the BTAs displayed in the fourth column of table 10 that satisfy condition (13).

Table 10: Results obtained from the application of the analytical method proposed in clause 4.3 to the radio link configuration 1

$\alpha_n \in \mathcal{A}$	β_n from equation (12)	Is constraint (13) satisfied?	BTA γ_n [%]
0,05	0,079	No	99,891
0,1	0,157	No	99,902
0,2	0,315	No	99,918
0,3	0,472	No	99,929
0,4	0,629	No	99,937
0,5	0,786	No	99,942
0,6	0,944	No	99,946
0,7	1,101	No	99,949
0,8	1,258	No	99,952
0,9	1,415	No	99,953
1	1,573	Yes	99,955
2	3,145	Yes	99,961
3	4,718	Yes	99,963
4	6,290	Yes	99,963
5	7,863	Yes	99,964
10	15,726	Yes	99,965
20	31,451	Yes	99,966
40	62,902	Yes	99,967
60	94,353	Yes	99,967
62	97,498	Yes	99,967
64	100,643	Yes	99,967
66	103,788	Yes	99,967
68	106,934	No	99,967
70	110,079	No	99,967

7 Conclusions

Planning backhaul networks through the New KPIs methodology calls for reliable techniques for predicting the traffic demand distributions across the different links, which are essential for accurately evaluating the novel BTA metric. The present document has introduced two complementary solutions to address this challenge.

The first method relies on an analytical procedure designed to estimate the worst-case BTA of any backhaul link. Its key advantage is that it is based solely on the knowledge of the average and peak values of the expected link traffic demand, rather than the full throughput statistical distribution. Although this approach inherently yields a conservative BTA evaluation, an experimental validation activity based on traffic time series collected from operational wireless transport networks has demonstrated its effectiveness in significantly reducing link over-engineering compared to current planning criteria.

The second method involves conducting measurement campaigns on live backhaul systems with the aim of deriving a dataset of traffic demand distributions to be possibly used as reference statistics for the assessment of the BTA in various deployment scenarios, with different environmental (e.g. in terms of topology and subscribers' density) and technological (e.g. in terms of transported RAN configurations) conditions.

It is worth noting that these two strategies can also be employed in a synergistic manner. In some cases, the data collected in real radio fixed networks could provide valuable insights into the traffic loads which may be expected in specific contexts of interest, that can in turn be used as inputs to the analytical procedure for computing worst-case (or lower bound) BTA values.

The contributions described in the present document - aimed at defining practical methodologies for assessing the BTA metric - are believed to represent a significant advancement in promoting and accelerating the adoption of the New KPIs-based design paradigm in current and future wireless backhaul networks.

Annex A: Experimental validation of the analytical procedure for deriving BTA lower bounds: methodology and results

A.1 Overview

Annex A provides a detailed description of the methodology used to define constraint (13) in the analytical procedure for deriving BTA lower bounds as illustrated in table 1.

As already mentioned in clause 4.3, inequality (13) limits the search of the BTA lower bounds within the subspace of (α, β) parameters that generate plausible traffic demand distributions where high throughput values occur with progressively smaller probabilities with respect to lower capacities, thus excluding, by way of example, the unrealistic behaviours previously highlighted in figures 4 and 5 (for $\beta = 0{,}5$ in figure 4-(a) and $\alpha = \beta = 0{,}5$ in figure 5-(a)). More specifically, this condition has been imposed by setting a restriction on the slope of the admissible cumulative distribution functions in the high-traffic region, and, in mathematical terms, it has been achieved by requiring that the maximum value of the derivative of the CDF $F_T(t, \alpha_n, \beta_n)$ produced by a generic pair of parameters (α_n, β_n) and evaluated at a traffic load equal to $\rho \times t_{max}$ (say with $0{,}9 \leq \rho \leq 1$) is upper-bounded by a convenient term η / t_{max}:

$$\left.\frac{\partial F_T(t,\alpha_n,\beta_n)}{\partial t}\right|_{t=\rho\times t_{max}} = f_T(t = \rho \times t_{max}, \alpha_n, \beta_n) = \frac{1}{t_{max}} \times \frac{(\rho)^{\alpha_n - 1}(1-\rho)^{\beta_n - 1}}{\Gamma(\alpha_n)\Gamma(\beta_n)}\Gamma(\alpha_n + \beta_n) \leq \frac{\eta}{t_{max}}, \quad \text{(A.1)}$$

where $f_T(t, \alpha_n, \beta_n)$ is the probability density function associated with the pair of parameters (α_n, β_n), and is given by equation (7).

The choice $\rho = 0{,}999$ and $\eta = 0{,}05$ for constraint (13) has been determined as a result of a thorough simulation campaign based on a dataset of traffic time series acquired from a currently operative backhaul network, as further detailed below.

The remainder of annex A is organized as follows. Clause A.2 provides an overview of the employed database, while clause A.3 describes the methodology adopted for the simulation activity, in terms of main assumptions, utilized metrics and test cases. Finally, clause A.4 discusses the numerical results.

A.2 Database description

The results described in annex A are based on a database composed of 1 510 time series obtained by recording the peak traffic loads of a set of links deployed in a commercial backhaul network for an overall period of 18 weeks, with a time resolution of 1 hour. It is remarked that this coarse data resolution (e.g. with respect to the 15 minutes time granularity typically supported by performance monitoring systems in currently deployed backhaul networks) does not constitute a limitation for the following analysis, since the real purpose of annex A is to numerically (and massively) assess how effectively the proposed analytical procedure is able to derive accurate lower bounds on the BTAs of transport links with arbitrary - yet realistic - traffic distributions, rather than to achieve a New-KPIs-compliant link planning (a process that would have undoubtedly involved managing traffic data with time resolutions on the order of 1 second, according to ETSI GR mWT 028 [i.1] and as discussed in different occasions within the present document).

In order to prevent the present study from being biased in favour of traffic distributions that would not be realistically and practically considered in any rationale backhaul link design process, the time series composing the above-mentioned database have been selected so as to:

- have a Peak-to-Average Ratio (PAR) lower than or equal to 8;
- have analytically continuous cumulative distribution functions;
- have cumulative distribution functions with probabilities higher than 99 % and 99,8 % for traffic values greater than $0{,}99 \times t_{max}$ and $0{,}998 \times t_{max}$ (being t_{max} the maximum value of each time series), respectively, thus ensuring a smooth behaviour in the high-throughput region (figure A.1 illustrates graphically this condition).

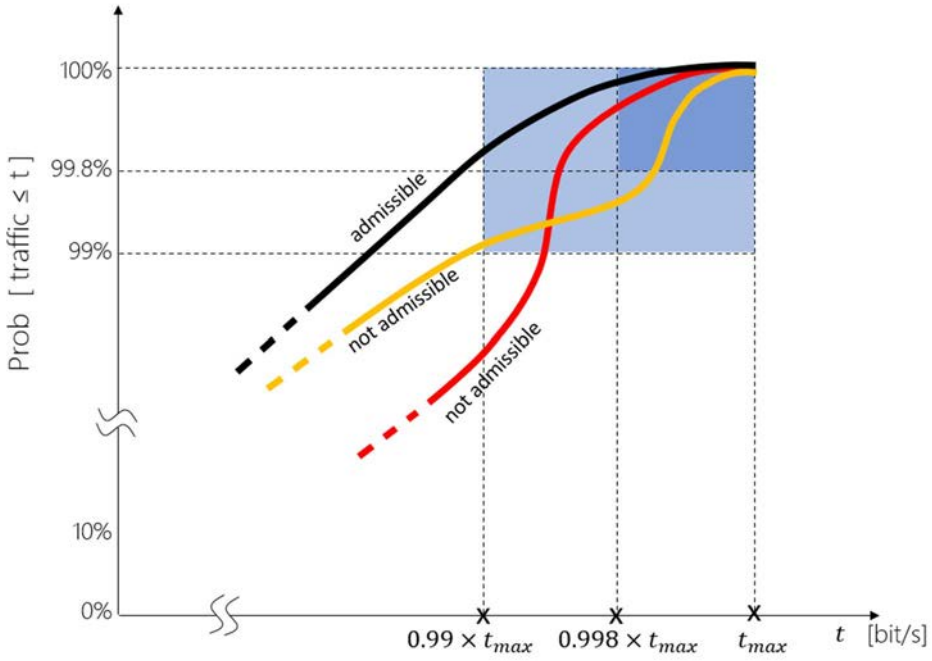

NOTE: Only the time series characterized by cumulative distribution functions with probabilities higher than 99 % and 99,8 % for traffic values greater than $0{,}99 \times t_{max}$ and $0{,}998 \times t_{max}$, respectively, have been included in the database.

Figure A.1: Graphical representation of the condition imposed on the cumulative distribution functions of the selected time series

A.3 Methodology, system assumptions and test cases

Each time series in the database described in clause A.2 has been re-scaled so as to have:

$$t_{max} = \omega \times C_{BH,max}, \tag{A.2}$$

where parameter $\omega < 1$ accounts for the unavoidable gap between the actual peak traffic value t_{max} and the maximum capacity $C_{BH,max}$ that can be delivered by the employed radio transport technology, and it will be varied in the different test cases considered in the present study. Backhaul links operating in E-band (at around 80 GHz) over a bandwidth of 500 MHz with vertically polarized electromagnetic field and supporting an ACM policy are here considered as the reference transport technology. More specifically, the analysis illustrated in clause A.4 will focus on five representative links, with hop lengths $d = 1, 2, 3, 4$ and 5 km, all deployed in a region with rainfall intensities exceeding 42 mm/h for 0,01 % of the time in a year.

A total of nine test datasets have been derived from the original database described in clause A.2:

Test dataset I: composed of all the traffic time series (i.e. with PAR ≤ 8), and selecting $\omega = 0{,}82$ in equation (A.2);

Test dataset II: composed of all the traffic time series, and selecting $\omega = 0{,}9$;

Test dataset III: composed of all the traffic time series, and selecting $\omega = 0{,}95$;

Test dataset IV: composed of the only traffic time series with PAR ≤ 6, and selecting $\omega = 0{,}82$;

Test dataset V: composed of the only traffic time series with PAR ≤ 6, and selecting $\omega = 0{,}9$;

Test dataset VI: composed of the only traffic time series with PAR ≤ 6, and selecting $\omega = 0{,}95$;

Test dataset VII: composed of the only traffic time series with PAR ≤ 4, and selecting $\omega = 0{,}82$;

Test dataset VIII: composed of the only traffic time series with PAR ≤ 4, and selecting $\omega = 0{,}9$;

Test dataset IX: composed of the only traffic time series with PAR ≤ 4, and selecting $\omega = 0{,}95$.

For each ith test dataset (i = I, II, III, IV, V, VI, VII, VIII, IX):

1) a cumulative distribution function has been first computed for each ℓth traffic time series, and has been then employed to generate, by applying equation (1), the **actual link BTA** value for each considered hop length d:

$$BTA_{\ell,d}(G_{tot})\ (\ell = 1,2, \dots, L_i;\ d = 1, 2, 3, 4, 5 \text{ km}), \tag{A.3}$$

where dependence on the overall antenna gain G_{tot} (namely, including both the receive and the transmit side), in dB, is explicitly indicated to facilitate the following description, while L_i is the total number of time series included in the ith test dataset.

NOTE 1: To derive the actual link BTAs, the availabilities of the different capacities offered by the radio connection for each hop length d have been computed on the basis of Recommendation ITU-R P.530-19 [i.4] by taking into account free-space loss, gaseous absorption and rain attenuation as the primary propagation impairments.

2) an average and a maximum traffic load value ($E[T]$ and t_{max}, respectively) have been derived for each ℓth traffic time series in the dataset, and have been employed as inputs to the analytical procedure as detailed in table 1, that has been run for each link distance d and for each kth choice of a pre-defined set of K pairs of parameters (ρ, η) to be used in constraint (13), in order to derive the corresponding **BTA lower bound**:

$$LB_{\ell,d,k}(G_{tot})\ (\ell = 1,2, \dots, L_i;\ d = 1, 2, 3, 4, 5 \text{ km};\ k = 1,2, \dots K). \tag{A.4}$$

The analysis presented in clause A.4 will evaluate all the combinations of $\rho \in \{0{,}99, 0{,}999, 0{,}9999, 0{,}99999\}$ and $\eta \in$ $\{0{,}002, 0{,}004, 0{,}006, 0{,}008, 0{,}01, 0{,}02, 0{,}03, 0{,}04, 0{,}05, 0{,}06, 0{,}07, 0{,}08, 0{,}09, 0{,}1, 0{,}2, 0{,}22, 0{,}24, 0{,}26, 0{,}28, 0{,}3, 0{,}32, 0{,}34, 0{,}36, 0{,}38, 0{,}4, 0{,}5, 0{,}6, 0{,}7, 0{,}8, 0{,}9, 1\}$, leading to an overall cardinality $K = 4 \times 31 = 124$.

3) a **relative error** between the derived BTA lower bound (step 2) and the actual link BTA (step 1) has been then computed for each ℓth time series, for each link distance d and for each kth pair (ρ_k, η_k) as:

$$\varepsilon_{\ell,d,k} = -\frac{(1 - BTA_{\ell,d}(G_{tot})) - (1 - LB_{\ell,d,k}(G_{tot}))}{(1 - BTA_{\ell,d}(G_{tot}))}. \tag{A.5}$$

NOTE 2: In formula (A.5), the relative error is expressed in terms of the outage quantities $(1 - BTA_{\ell,d}(G_{tot}))$ and $(1 - LB_{\ell,d,k}(G_{tot}))$.

4) an **excess gain** $\Delta_{\ell,d,k}$ in dB needed to achieve a BTA lower bound $LB_{\ell,d,k}$ numerically equal to the actual link BTA $BTA_{\ell,d}$ has been computed for each ℓth time series, for each link distance d and for each kth pair (ρ_k, η_k). In mathematical notation, excess gain $\Delta_{\ell,d,k}$ guarantees that:

$$LB_{\ell,d,k}\left(G_{tot} + \Delta_{\ell,d,k}\right) = BTA_{\ell,d}(G_{tot}). \tag{A.6}$$

It is highlighted that the latter metric has the scope of quantifying, in [dB], the superfluous system margin that the employment of the proposed analytical procedure for deriving BTA lower bounds with parameters (ρ_k, η_k) would introduce in a possible planning process involving a link with length d and carrying a traffic expressed by the ℓth time series.

In clause A.4, the best pair of parameters (ρ, η) is investigated for every ith test dataset on the basis of an assessment of the following three key metrics:

1) the statistical distribution of the relative errors $\varepsilon_{\ell,d,k}$ derived for all the L_i time series and the five link distances under consideration;

2) the statistical distribution of the excess gains $\Delta_{\ell,d,k}$ derived for all the L_i time series and the five link distances under consideration;

3) the **lower bound efficiency** v_k, defined as the percentage of cases in which the proposed analytical procedure employing the kth pair (ρ_k, η_k) in constraint (13) succeeds in generating actual BTA lower bounds. Since, according to equation (A.5), $LB_{\ell,d,k}(G_{tot})$ constitutes a lower bound on the actual link BTA value computed for each ℓth time series and for each link distance d if and only if $\varepsilon_{\ell,d,k} \geq 0$, it yields:

$$v_k = \frac{1}{L_i \times 5} \sum_{\ell=1}^{L_i} \sum_{d=1}^{5\text{ km}} \mathbf{1}\left(\varepsilon_{\ell,d,k}\right) \times 100 \quad [\%], \tag{A.7}$$

where $\mathbf{1}(x)$ is the step function, defined as:

$$\mathbf{1}(x) = \begin{cases} 1 \; if \; x \geq 0 \\ 0 \; if \; x < 0 \end{cases} \tag{A.8}$$

A.4 Numerical results

The numerical results obtained for Test datasets I through IX are summarized in tables A.2 through A.10, respectively, which show, for each kth choice of the pair of parameters (ρ, η) (i.e. for each kth row):

i) the lower bound efficiency v_k (third column);

ii) the minimum relative error experienced over all the L_i time series and the five link distances (fourth column); and

iii) the median (fifth column), the 75th percentile (sixth column), the 90th percentile (seventh column), the 95th percentile (eighth column) and the 99th percentile (ninth column) of the statistical distribution of the excess gains $\Delta_{\ell,d,k}$ derived for all the L_i time series and the five link distances (i.e. $\ell = 1,2, \ldots, L_i$ and $d = 1,2,3,4,5$ km).

It is observed that, according to equation (A.5), the minimum relative error in the fourth column is negative whenever the efficiency metric v_k is strictly lower than 100 %, and in those cases it provides an important indication of the extent to which an actual link BTA value can fall below the BTA lower bound computed according to the proposed method with the kth pair (ρ_k, η_k) used in constraint (13).

NOTE: For conciseness, tables A.2 through A.10 only report a sub-selection of the analysed values of parameters (ρ, η).

Tables A.2 through A.10 illustrate that employing the analytical procedure with relaxed conditions on constraint (13) (for example, in rows 3-4 of table A.2) guarantees to find actual BTA lower bounds for all the links (v_k = 100 %), at the expense of a generally high excess gain (larger than 5 dB in 50 % of cases in the considered examples). At the same time, the results suggest that the inherent trade-off between lower bound tightness and overall accuracy can be optimized by pursuing the reasonable compromise of selecting pairs of parameters (ρ, η) that could cause a slight degradation in the lower bound efficiency v_k (with respect to the full scale of 100 %), while yielding the advantage of maintaining the excess gain below 3 dB in the majority (i.e. in the range 95 % to 99 %) of cases. It is remarked that the 3 dB value is compatible with the margin that is typically considered in network planning phases to compensate for unexpected system losses along the transmission links, such as those caused by misalignments between transmit and receive antennas due to imperfect installation. Accordingly, in the present document the optimum pair (ρ, η) is defined as the one that results in the minimum 95th percentile value of the excess gain across all test cases, while simultaneously guaranteeing the following two conditions:

C1 lower bound efficiency v_k always higher than 99 %;

C2 minimum relative error experienced in all test cases higher than -21 % (it is recalled that the relative error is negative only when the BTA lower bound value is higher than the actual link BTA, according to equation (A.5)).

It is noted that conditions **C1** and **C2** imply that the proposed analytical procedure can fail to compute an actual lower bound in only 1 % of the cases within the considered datasets, and that, in such rare circumstances, the BTA lower bound can exceed the actual link BTA by only a very limited amount. To illustrate this quantitatively, table A.1 reports, for each BTA lower bound value shown in the first column, the minimum actual link BTA that could result according to condition **C2** and equation (A.5).

Table A.1: BTA lower bounds and corresponding minimum actual link BTAs according to condition C2

BTA lower bound [%]	Minimum actual link BTA [%]
99,9	99,873418
99,95	99,936709
99,99	99,987342
99,995	99,993671
99,999	99,998734

Considering all the analysed test cases, the optimum pair of parameters (ρ, η) that minimizes the 95th percentile value of the excess gain and that at the same time guarantees conditions **C1** and **C2** turns out to be:

$$\rho = 0{,}999,\ \eta = 0{,}05, \tag{A.9}$$

and this is the recommended choice for the application of the analytical procedure in table 1 of clause 4.3.

Table A.2: Selected results for Test dataset I (PAR ≤ 8, ω = 0,82)

ρ	η	LB efficiency ν_k [%]	minimum relative error [%]	Excess gain [dB]				
				50-percentile	75-percentile	90-percentile	95-percentile	99-percentile
0.99	0.01	93.59	-20.99	0.68	1.07	1.46	1.55	3.01
0.99	0.02	95.32	-19.65	0.78	1.15	1.47	1.59	3.04
0.99	0.9	100.00	45.85	5.22	5.55	6.16	7.73	9.15
0.99	1	100.00	45.85	5.22	5.55	6.16	7.73	9.15
0.999	0.02	98.01	-13.82	1.01	1.40	1.49	1.67	3.06
0.999	0.04	98.98	-12.45	1.15	1.42	1.50	1.72	3.06
0.999	**0.05**	**99.05**	**-10.92**	**1.17**	**1.43**	**1.54**	**1.77**	**3.07**
0.999	0.06	99.17	-10.92	1.17	1.43	1.57	1.81	3.07
0.999	0.08	99.30	-9.18	1.27	1.44	1.61	1.86	3.07
0.999	0.1	99.32	-9.18	1.32	1.45	1.65	1.90	3.07
0.9999	0.002	97.30	-15.05	0.88	1.30	1.48	1.62	3.05
0.9999	0.004	97.66	-13.82	0.98	1.37	1.49	1.65	3.05
0.9999	0.006	97.87	-12.45	1.03	1.40	1.49	1.67	3.06
0.99999	0.002	97.83	-12.45	1.05	1.41	1.49	1.67	3.06
0.99999	0.004	98.29	-10.92	1.12	1.42	1.50	1.71	3.06
0.99999	0.006	98.65	-10.92	1.17	1.43	1.53	1.75	3.06

Table A.3: Selected results for Test dataset II (PAR ≤ 8, ω = 0,9)

ρ	η	LB efficiency ν_k [%]	minimum relative error [%]	Excess gain [dB]				
				50-percentile	75-percentile	90-percentile	95-percentile	99-percentile
0.99	0.01	95.05	-27.52	0.88	1.18	1.46	1.49	3.00
0.99	0.02	96.54	-25.89	0.99	1.29	1.47	1.57	3.03
0.99	0.9	100.00	136.36	8.69	9.05	10.61	10.76	12.34
0.99	1	100.00	136.36	8.69	9.05	10.61	10.76	12.34
0.999	0.02	99.10	-18.79	1.37	1.47	1.70	1.99	3.06
0.999	0.04	99.47	-18.52	1.49	1.55	1.90	2.22	3.07
0.999	**0.05**	**99.47**	**-18.52**	**1.56**	**1.61**	**1.97**	**2.27**	**3.07**
0.999	0.06	99.50	-15.00	1.56	1.66	2.03	2.30	3.07
0.999	0.08	99.62	-13.55	1.56	1.77	2.16	2.43	3.08
0.999	0.1	99.63	-13.55	1.56	1.84	2.23	2.56	3.08
0.9999	0.002	98.64	-22.04	1.22	1.44	1.59	1.82	3.05
0.9999	0.004	98.65	-22.04	1.32	1.46	1.67	1.93	3.05
0.9999	0.006	98.82	-18.52	1.37	1.47	1.73	2.00	3.06
0.99999	0.002	98.79	-18.52	1.37	1.48	1.77	2.05	3.06
0.99999	0.004	99.27	-18.52	1.46	1.52	1.88	2.21	3.06
0.99999	0.006	99.40	-18.52	1.51	1.57	1.94	2.25	3.07

Table A.4: Selected results for Test dataset III (PAR ≤ 8, ω = 0,95)

ρ	η	LB efficiency ν_k [%]	minimum relative error [%]	Excess gain [dB]				
				50-percentile	75-percentile	90-percentile	95-percentile	99-percentile
0.99	0.01	95.66	-40.88	1.12	1.41	1.50	1.68	3.02
0.99	0.02	97.31	-38.67	1.32	1.47	1.71	1.92	3.04
0.99	0.9	100.00	106.04	8.20	8.64	9.15	10.63	12.30
0.99	1	100.00	106.04	8.20	8.64	9.15	10.63	12.30
0.999	0.02	99.39	-27.37	1.56	1.96	2.31	2.62	3.07
0.999	0.04	99.64	-24.34	1.86	2.22	2.58	3.00	3.09
0.999	**0.05**	**99.70**	**-20.79**	**1.95**	**2.27**	**2.69**	**3.02**	**3.09**
0.999	0.06	99.70	-20.79	2.01	2.30	2.79	3.03	3.10
0.999	0.08	99.80	-16.60	2.15	2.45	2.97	3.06	3.19
0.999	0.1	99.80	-16.60	2.25	2.56	3.02	3.07	3.29
0.9999	0.002	99.10	-29.97	1.56	1.72	2.13	2.33	3.05
0.9999	0.004	99.22	-27.37	1.56	1.89	2.26	2.52	3.06
0.9999	0.006	99.30	-24.34	1.56	1.98	2.33	2.65	3.07
0.99999	0.002	99.23	-24.34	1.61	2.00	2.36	2.69	3.07
0.99999	0.004	99.55	-20.79	1.76	2.17	2.53	2.91	3.09
0.99999	0.006	99.59	-20.79	1.86	2.23	2.62	3.01	3.09

Table A.5: Selected results for Test dataset IV (PAR ≤ 6, ω = 0,82)

ρ	η	LB efficiency ν_k [%]	minimum relative error [%]	Excess gain [dB]				
				50-percentile	75-percentile	90-percentile	95-percentile	99-percentile
0.99	0.01	95.16	-20.98	0.73	1.10	1.46	1.53	1.89
0.99	0.02	96.82	-19.64	0.78	1.18	1.47	1.55	1.99
0.99	0.9	100.00	48.61	5.27	5.56	6.15	7.65	9.10
0.99	1	100.00	48.61	5.27	5.56	6.15	7.65	9.10
0.999	0.02	99.25	-13.81	1.07	1.40	1.49	1.62	3.01
0.999	0.04	99.66	-12.45	1.17	1.42	1.50	1.67	3.03
0.999	**0.05**	**99.66**	**-10.91**	**1.20**	**1.43**	**1.52**	**1.69**	**3.04**
0.999	0.06	99.66	-10.91	1.25	1.44	1.55	1.72	3.05
0.999	0.08	99.68	-9.18	1.29	1.45	1.59	1.78	3.05
0.999	0.1	99.69	-9.18	1.37	1.46	1.63	1.82	3.05
0.9999	0.002	98.90	-15.04	0.98	1.31	1.48	1.59	2.22
0.9999	0.004	99.18	-13.81	1.03	1.38	1.48	1.61	2.28
0.9999	0.006	99.34	-12.45	1.07	1.40	1.49	1.63	3.01
0.99999	0.002	99.37	-12.45	1.07	1.41	1.49	1.64	3.01
0.99999	0.004	99.57	-10.91	1.17	1.42	1.50	1.67	3.02
0.99999	0.006	99.66	-10.91	1.17	1.43	1.51	1.69	3.03

Table A.6: Selected results for Test dataset V (PAR ≤ 6, ω = 0,9)

ρ	η	LB efficiency ν_k [%]	minimum relative error [%]	Excess gain [dB]				
				50-percentile	75-percentile	90-percentile	95-percentile	99-percentile
0.99	0.01	95.90	-27.50	0.90	1.20	1.46	1.49	1.79
0.99	0.02	97.07	-25.88	1.05	1.31	1.47	1.52	1.88
0.99	0.9	100.00	137.76	8.74	9.06	9.97	10.72	12.29
0.99	1	100.00	137.76	8.74	9.06	9.97	10.72	12.29
0.999	0.02	99.44	-18.78	1.37	1.48	1.69	1.91	3.02
0.999	0.04	99.66	-18.62	1.54	1.56	1.88	2.10	3.04
0.999	**0.05**	**99.66**	**-18.62**	**1.56**	**1.62**	**1.94**	**2.20**	**3.05**
0.999	0.06	99.66	-14.99	1.56	1.67	1.99	2.24	3.05
0.999	0.08	99.71	-13.63	1.56	1.77	2.11	2.29	3.06
0.999	0.1	99.71	-13.63	1.56	1.85	2.21	2.37	3.06
0.9999	0.002	99.38	-22.15	1.27	1.44	1.59	1.77	2.26
0.9999	0.004	99.40	-22.15	1.37	1.46	1.66	1.87	2.45
0.9999	0.006	99.47	-18.62	1.37	1.48	1.73	1.94	3.01
0.99999	0.002	99.56	-18.62	1.42	1.48	1.76	1.97	3.01
0.99999	0.004	99.63	-18.62	1.50	1.53	1.87	2.08	3.03
0.99999	0.006	99.69	-18.62	1.56	1.58	1.92	2.17	3.04

Table A.7: Selected results for Test dataset VI (PAR ≤ 6, ω = 0,95)

ρ	η	LB efficiency ν_k [%]	minimum relative error [%]	Excess gain [dB]				
				50-percentile	75-percentile	90-percentile	95-percentile	99-percentile
0.99	0.01	95.96	-40.87	1.17	1.41	1.50	1.65	2.01
0.99	0.02	97.56	-38.66	1.37	1.47	1.70	1.88	2.28
0.99	0.9	100.00	105.10	8.25	8.65	9.13	9.91	10.78
0.99	1	100.00	105.10	8.25	8.65	9.13	9.91	10.78
0.999	0.02	99.56	-27.37	1.64	1.99	2.29	2.53	3.05
0.999	0.04	99.75	-24.34	1.90	2.23	2.56	2.88	3.08
0.999	**0.05**	**99.75**	**-20.79**	**1.95**	**2.27**	**2.66**	**3.00**	**3.09**
0.999	0.06	99.75	-20.79	2.05	2.31	2.75	3.02	3.10
0.999	0.08	99.78	-16.60	2.16	2.45	2.93	3.05	3.20
0.999	0.1	99.78	-16.60	2.29	2.56	3.01	3.07	3.30
0.9999	0.002	99.50	-29.97	1.56	1.74	2.12	2.29	3.00
0.9999	0.004	99.63	-27.37	1.56	1.90	2.25	2.44	3.03
0.9999	0.006	99.63	-24.34	1.66	2.00	2.30	2.56	3.06
0.99999	0.002	99.66	-24.34	1.66	2.03	2.34	2.60	3.06
0.99999	0.004	99.75	-20.79	1.81	2.20	2.51	2.79	3.08
0.99999	0.006	99.75	-20.79	1.94	2.24	2.59	2.92	3.09

Table A.8: Selected results for Test dataset VII (PAR ≤ 4, ω = 0,82)

ρ	η	LB efficiency ν_k [%]	minimum relative error [%]	Excess gain [dB]				
				50-percentile	75-percentile	90-percentile	95-percentile	99-percentile
0.99	0.01	94.97	-21.08	0.79	1.26	1.48	1.61	1.87
0.99	0.02	96.63	-19.73	0.88	1.28	1.48	1.61	1.87
0.99	0.9	100.00	50.07	5.30	5.68	6.16	6.19	7.75
0.99	1	100.00	50.07	5.30	5.68	6.16	6.19	7.75
0.999	0.02	99.27	-13.88	1.17	1.42	1.49	1.63	1.88
0.999	0.04	99.58	-12.50	1.27	1.44	1.53	1.66	1.89
0.999	**0.05**	**99.58**	**-10.96**	**1.32**	**1.44**	**1.56**	**1.68**	**1.91**
0.999	0.06	99.58	-10.96	1.37	1.45	1.58	1.69	1.93
0.999	0.08	99.58	-9.23	1.37	1.46	1.61	1.73	1.97
0.999	0.1	99.58	-9.23	1.42	1.47	1.64	1.78	2.03
0.9999	0.002	99.13	-15.11	1.10	1.40	1.49	1.62	1.88
0.9999	0.004	99.38	-13.88	1.17	1.42	1.49	1.63	1.88
0.9999	0.006	99.46	-12.50	1.17	1.42	1.50	1.64	1.88
0.99999	0.002	99.52	-12.50	1.20	1.43	1.50	1.65	1.88
0.99999	0.004	99.56	-10.96	1.27	1.44	1.54	1.67	1.90
0.99999	0.006	99.58	-10.96	1.32	1.45	1.57	1.68	1.92

Table A.9: Selected results for Test dataset VIII (PAR ≤ 4, ω = 0,9)

ρ	η	LB efficiency ν_k [%]	minimum relative error [%]	Excess gain [dB]				
				50-percentile	75-percentile	90-percentile	95-percentile	99-percentile
0.99	0.01	94.78	-27.57	1.00	1.26	1.46	1.50	1.82
0.99	0.02	96.26	-25.94	1.15	1.37	1.48	1.59	1.85
0.99	0.9	100.00	136.37	8.79	9.09	9.88	10.63	10.77
0.99	1	100.00	136.37	8.79	9.09	9.88	10.63	10.77
0.999	0.02	99.29	-18.82	1.46	1.49	1.75	1.92	2.24
0.999	0.04	99.52	-18.55	1.56	1.63	1.92	2.10	2.30
0.999	**0.05**	**99.52**	**-18.55**	**1.56**	**1.68**	**1.97**	**2.17**	**2.38**
0.999	0.06	99.52	-15.03	1.56	1.73	2.02	2.22	2.43
0.999	0.08	99.58	-13.57	1.56	1.82	2.12	2.26	2.50
0.999	0.1	99.58	-13.57	1.61	1.89	2.21	2.29	2.60
0.9999	0.002	99.29	-22.06	1.37	1.46	1.65	1.81	2.10
0.9999	0.004	99.31	-22.06	1.44	1.48	1.72	1.89	2.23
0.9999	0.006	99.42	-18.55	1.49	1.50	1.80	1.96	2.26
0.99999	0.002	99.46	-18.55	1.51	1.53	1.83	1.99	2.28
0.99999	0.004	99.50	-18.55	1.56	1.63	1.92	2.11	2.31
0.99999	0.006	99.56	-18.55	1.56	1.67	1.97	2.18	2.38

Table A.10: Selected results for Test dataset IX (PAR ≤ 4, ω = 0,95)

ρ	η	LB efficiency ν_k [%]	minimum relative error [%]	Excess gain [dB]				
				50-percentile	75-percentile	90-percentile	95-percentile	99-percentile
0.99	0.01	94.72	-40.91	1.22	1.43	1.57	1.71	2.00
0.99	0.02	96.69	-38.71	1.37	1.49	1.76	1.92	2.24
0.99	0.9	100.00	106.61	8.30	8.66	9.10	9.18	9.97
0.99	1	100.00	106.61	8.30	8.66	9.10	9.18	9.97
0.999	0.02	99.46	-27.40	1.76	2.06	2.30	2.50	2.86
0.999	0.04	99.65	-24.37	1.95	2.25	2.56	2.76	3.07
0.999	**0.05**	**99.65**	**-20.81**	**2.05**	**2.29**	**2.64**	**2.85**	**3.09**
0.999	0.06	99.65	-20.81	2.15	2.33	2.71	2.93	3.15
0.999	0.08	99.69	-16.62	2.25	2.46	2.85	3.03	3.26
0.999	0.1	99.69	-16.62	2.34	2.58	2.99	3.07	3.35
0.9999	0.002	99.38	-30.00	1.56	1.87	2.22	2.30	2.66
0.9999	0.004	99.56	-27.40	1.66	2.00	2.28	2.45	2.80
0.9999	0.006	99.56	-24.37	1.76	2.09	2.36	2.55	2.93
0.99999	0.002	99.60	-24.37	1.76	2.13	2.40	2.59	2.97
0.99999	0.004	99.65	-20.81	1.95	2.24	2.54	2.74	3.07
0.99999	0.006	99.65	-20.81	2.00	2.27	2.61	2.82	3.09

Annex B:
A methodology for analysing the impacts of New KPIs on Total Cost of Ownership

The aim of the present annex B is to illustrate a methodology for obtaining a general assessment of the benefits, in terms of cost of ownership, brought by the New KPIs paradigm. The envisioned approach starts by identifying a target backhaul network and a desired peak capacity that needs to be transported over each link (for the sake of simplicity - and without affecting the validity of the presented methodology - a unique peak capacity value for all the links is here considered). Based on these inputs, the cost savings enabled by the New KPIs planning methodology - with respect to traditional designs - can be evaluated according to the following step-by-step procedure:

1) derive the statistical distribution of the link lengths of the target backhaul network with a predefined granularity, e.g. obtaining a relative frequency histogram qualitatively similar to the one shown in figure B.1 (therein with 1 km granularity);

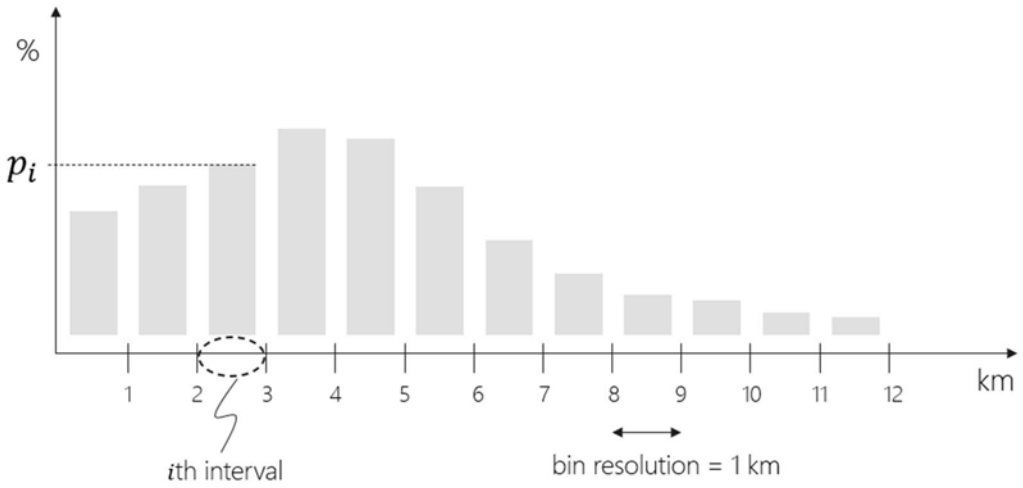

NOTE: This figure illustrates the percentages p_i of links spanning a distance that falls within each *i*th interval (for $i = 1, 2, \ldots, 12$).

Figure B.1: Qualitative representation of the relative frequency histogram of link lengths in the target backhaul network

2) identify a set of preferred transport technologies that are able to deliver the desired peak capacities;

3) define the target conditions for both the traditional and the New KPIs planning methodologies. By way of example, table B.1 shows a possible set of objectives to be guaranteed for the two approaches;

4) for each transport technology as selected in step 2, identify the maximum link distances that can be achieved by employing both the traditional and the New KPIs planning methodologies;

5) compute the Total Cost of Ownership (TCO) of the target backhaul network planned according to the traditional planning methodology as:

$$TCO = \sum_{i=1}^{I} c_i \times p_i, \quad \text{(B.1)}$$

where index i varies across the I resolvable intervals of the link lengths distribution as derived in step 1 ($I = 12$ in the example of figure B.1), c_i is the cost of the least expensive transport technology that can be employed to cover all the connection distances included in the *i*th interval while satisfying the target conditions (e.g. those outlined in the first row of table B.1), while p_i is the relative number of links in the network with distances included in the *i*th interval (see figure B.1 for a graphical representation);

6) similarly to step 5, compute the TCO of the target network planned according to the New KPIs methodology as:

$$TCO_{New\ KPIs} = \sum_{i=1}^{I} \tilde{c}_i \times p_i; \quad \text{(B.2)}$$

7) compare the TCOs derived at steps 5 and 6 to determine the cost savings enabled by the New KPIs planning methodology.

NOTE: Within each ith link lengths interval, the set of the eligible transport technologies depends on the maximum distance thresholds derived in step 4, therefore $\tilde{c}_i$ generally differs from parameter c_i used in step 5.

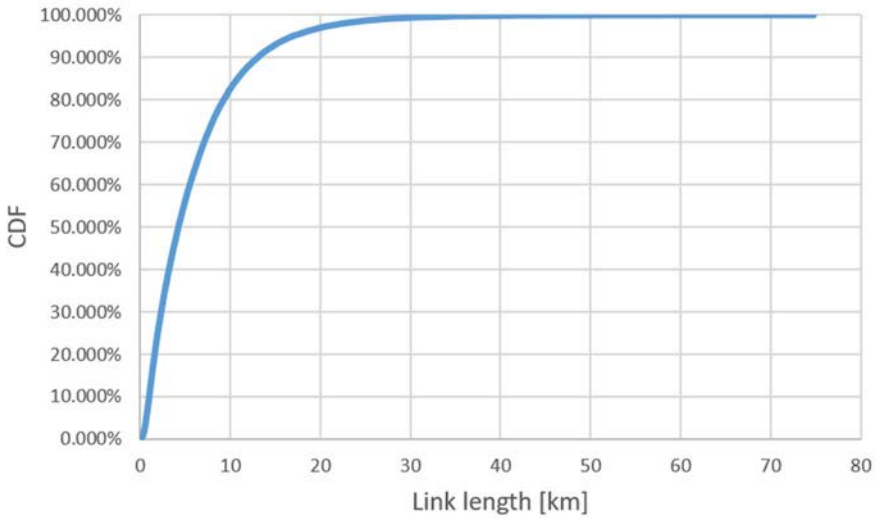

Figure B.2: Link lengths distribution of the backhaul network analysed as example in the present annex B

Table B.1: Target conditions for the traditional and New KPIs planning methodologies considered in the present annex B

	Target conditions
Traditional planning	• ≥ 99,995 % availability for a capacity representing 15 % to 20 % of the desired peak capacity • ≥ 5 dB fade margin for the modulation format providing the desired peak capacity
New KPIs planning	• ≥ 99,995 % availability for a capacity at least equal to 200 Mbit/s • ≥ 99,9 % BTA • ≥ 5 dB fade margin for the modulation format providing the desired peak capacity

For the sake of clarity, the remaining part of the present annex B will apply the procedure described above to assess the potential savings - in terms of costs related to the yearly spectrum license fees only - enabled by the New KPIs paradigm. Towards this goal, a hypothetical backhaul network characterized by a link lengths distribution as shown in figure B.2 is considered, and two target European deployment regions are taken into account, with rainfall intensities exceeding either 32 mm/h or 42 mm/h for 0,01 % of the time in a year (these will be referred to in the following as 32 mm/h and 42 mm/h rain intensity zones, respectively, for simplicity).

Pursuing a desired peak capacity of 4 Gbit/s for all the connections, three backhaul solutions have been selected as candidate technologies:

- an **E-band** point-to-point system with 250 MHz bandwidth and dual polarization;
- a **Dual Band** point-to-point system operating on both E-band (250 MHz bandwidth, dual polarization) and 18 GHz frequency band (56 MHz bandwidth, dual polarization);

- an **18 GHz** point-to-point system aggregating two 112 MHz channels and operating with dual polarization.

Tables B.2 and B.3 quantify the maximum link lengths achievable by the three different transport technologies described above for 32 mm/h and 42 mm/h rain intensity zones, respectively, considering the target conditions shown in table B.1 (it is remarked that, in the present analysis, the assessment of the BTA has been based on the analytical procedure detailed in table 1 for all the links). Based on these results, the numerical evaluations that follow have been limited to the subset of links spanning a distance lower than or equal to 10,5 km and 10 km for the 32 mm/h and 42 mm/h rain intensity zones, respectively, which represent the largest achievable hop lengths under the traditional planning methodology in the two cases.

The New KPIs, enabling a wider adoption of both the E-band and the Dual Band technologies compared to traditional planning approaches, position themselves as the most favourable metrics for reducing the overall spectrum-related expenditures in scenarios where yearly license fees are inversely proportional to the operational frequency - a characteristic that applies to the majority of cases in today's backhaul markets (by way of example, table B.4 reports the per-link annual spectrum costs for the three backhaul technologies under inspection in two European Countries). In line with this consideration, the present analysis has revealed significant savings of:

- 22 % and 26 % in the 32 mm/h rain intensity zone when considering the per-link yearly spectrum license fees of EU Country 1 and 2 in table B.4, respectively;

- 28 % and 35 % in the 42 mm/h rain intensity zone when considering the per-link yearly spectrum license fees of EU Country 1 and 2, respectively.

It is also observed that, compared to backhaul technologies operating at lower frequencies, E-band systems require fewer radio channels to achieve the same delivered capacities, thanks to their significantly larger available bandwidths. Consequently, the adoption of the New KPIs approach - which extends the E-band usability range - offers the additional benefit of a more cost-effective deployment due to the generally reduced amount of hardware to be installed.

Table B.2: Maximum achievable link lengths with traditional and New KPIs planning methodologies for 32 mm/h rain intensity zone

	Traditional planning	New KPIs planning
E-band	4,2 km	5,3 km
Dual Band	8,8 km	14,3 km
18 GHz	10,5 km	10,5 km

Table B.3: Maximum achievable link lengths with traditional and New KPIs planning methodologies for 42 mm/h rain intensity zone

	Traditional planning	New KPIs planning
E-band	3,3 km	4,2 km
Dual Band	7 km	11,5 km
18 GHz	10 km	10,5 km

Table B.4: Per-link annual spectrum license fees for the three backhaul technologies under inspection in two European Countries

	EU Country 1	EU Country 2
E-band	575 €	1 614 €
Dual Band	1 955 €	4 924 €
18 GHz	3 850 €	12 841 €

Annex C:
Method for determining the target BTAs on individual links in tree-shaped backhaul network topologies

C.1 Method for a simple network topology

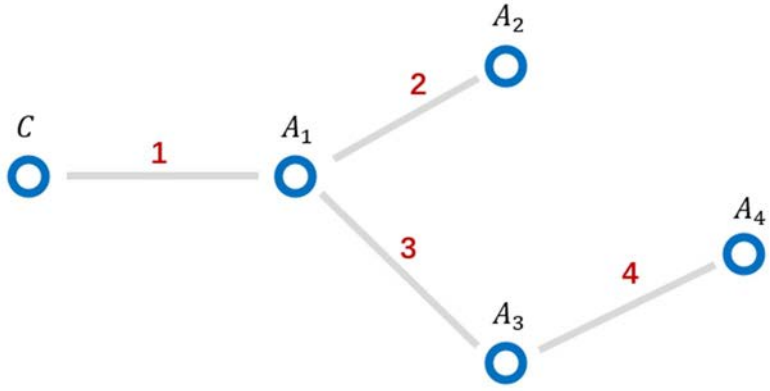

Figure C.1: Backhaul network topology analysed in the present clause C.1

The present annex C focuses on the network topology illustrated in figure C.1, where four radio sites:

$$A_1,\ A_2,\ A_3,\ A_4$$

are connected to a common aggregation node C via the distinct sets of links:

$$\mathcal{L}_1 = \{1\}, \mathcal{L}_2 = \{2,1\}, \mathcal{L}_3 = \{3,1\}, \mathcal{L}_4 = \{4,3,1\},$$

respectively. It is assumed that the transport network under consideration needs to be planned to ensure that the traffic generated by each radio site A_k ($k = 1,2,3,4$) and directed to node C achieves an end-to-end (i.e. over the whole cascade of connections belonging to set $\mathcal{L}_k$) BTA equal to ξ_k. To meet these conditions, the target BTAs of the different backhaul links should satisfy the set of inequalities obtained by applying the BTA apportionment rule for daisy-chain topologies as described in annex A of ETSI GR mWT 028 [i.1] successively to all radio sites. More specifically, in the scenario of figure C.1:

- radio site A_1 is connected to the aggregation node C exclusively via link 1. Consequently, to meet the constraint on the objective end-to-end BTA ξ_1, link 1 should be designed to achieve a target Backhaul Traffic Availability $\overline{BTA}_1$ such that:

$$(1 - \overline{BTA}_1) \leq (1 - \xi_1); \quad \text{(C.1)}$$

- radio site A_2 reaches node C through links 2 and 1. Therefore, the target BTAs for link 2 and link 1, denoted as $\overline{BTA}_2$ and $\overline{BTA}_1$, respectively, should satisfy the following inequality:

$$(1 - \overline{BTA}_2) + (1 - \overline{BTA}_1) \leq (1 - \xi_2); \quad \text{(C.2)}$$

- radio site A_3 is connected to node C via links 3 and 1. The corresponding target BTAs - $\overline{BTA}_3$ and $\overline{BTA}_1$ - should then satisfy:

$$(1 - \overline{BTA}_3) + (1 - \overline{BTA}_1) \leq (1 - \xi_3); \quad \text{(C.3)}$$

- radio site A_4 communicates with node C through links 4, 3, and 1. The target BTAs for links 4, 3 and 1 - namely $\overline{BTA}_4$, $\overline{BTA}_3$ and $\overline{BTA}_1$ - should satisfy:

$$(1 - \overline{BTA}_4) + (1 - \overline{BTA}_3) + (1 - \overline{BTA}_1) \leq (1 - \xi_4). \quad \text{(C.4)}$$

Any selection of the target link BTAs - $\overline{BTA}_1$, $\overline{BTA}_2$, $\overline{BTA}_3$ and $\overline{BTA}_4$ - that satisfies the constraints in inequalities (C.1) through (C.4) ensures a valid network design capable of meeting the desired end-to-end Backhaul Traffic Availability levels ξ_1, ξ_2, ξ_3 and ξ_4 for the data flows generated by each node.

When a uniform BTA apportionment is applied across the sequence of links connecting each radio site to the aggregation node C, the inequalities (C.1) through (C.4) result in the following constraints on the individual target link BTAs $\{\overline{BTA}_k\}_{k=1}^4$:

- for A_1 (single link):

$$(1 - \overline{BTA}_1) \leq (1 - \xi_1) \tag{C.5}$$

- for A_2 (two links):

$$(1 - \overline{BTA}_1) \leq \frac{(1 - \xi_2)}{2}, \qquad (1 - \overline{BTA}_2) \leq \frac{(1 - \xi_2)}{2} \tag{C.6}$$

- for A_3 (two links):

$$(1 - \overline{BTA}_1) \leq \frac{(1 - \xi_3)}{2}, \qquad (1 - \overline{BTA}_3) \leq \frac{(1 - \xi_3)}{2} \tag{C.7}$$

- for A_4 (three links):

$$(1 - \overline{BTA}_1) \leq \frac{(1 - \xi_4)}{3}, \qquad (1 - \overline{BTA}_3) \leq \frac{(1 - \xi_4)}{3}, \qquad (1 - \overline{BTA}_4) \leq \frac{(1 - \xi_4)}{3}. \tag{C.8}$$

Based on constraints (C.5) through (C.8), the individual target link BTAs can be selected as follows:

- for link 1, which is shared across all four radio sites, the most stringent constraint applies. Therefore:

$$(1 - \overline{BTA}_1) = min\left((1 - \xi_1), \frac{(1 - \xi_2)}{2}, \frac{(1 - \xi_3)}{2}, \frac{(1 - \xi_4)}{3}\right) \tag{C.9}$$

- for link 2, used only by radio site A_2:

$$(1 - \overline{BTA}_2) = \frac{(1 - \xi_2)}{2} \tag{C.10}$$

- for link 3, shared by sites A_3 and A_4:

$$(1 - \overline{BTA}_3) = min\left(\frac{(1 - \xi_3)}{2}, \frac{(1 - \xi_4)}{3}\right) \tag{C.11}$$

- for link 4, used exclusively by site A_4:

$$(1 - \overline{BTA}_4) = \frac{(1 - \xi_4)}{3}. \tag{C.12}$$

By applying equations (C.9) through (C.12), the network designer can determine the appropriate target BTAs for each individual link to ensure that the overall end-to-end Backhaul Traffic Availability conditions ξ_1, ξ_2, ξ_3 and ξ_4 are met for all the radio sites. Figure C.2 illustrates the resulting individual target BTAs for the case $\xi_1 = \xi_2 = \xi_3 = \xi_4 = 99{,}9$ %.

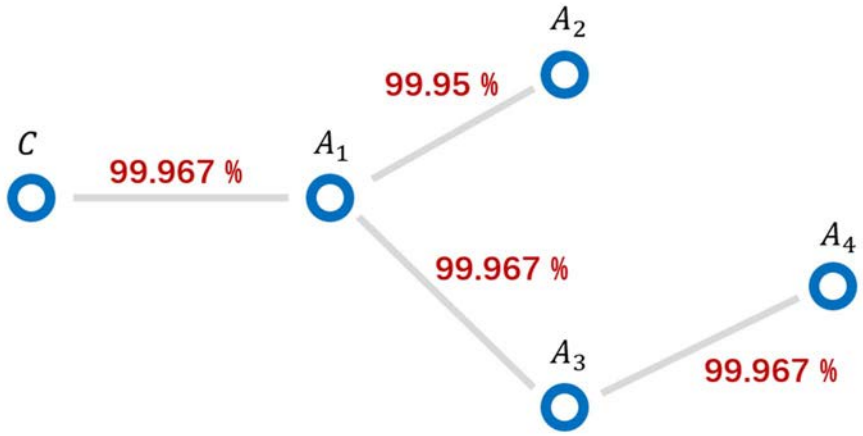

Figure C.2: Illustrative target BTAs for the individual links of the network topology in figure C.1 when $\xi_1 = \xi_2 = \xi_3 = \xi_4$ = 99,9 % and with uniform BTA apportionment strategy

C.2 Method for all network topologies

The method outlined in clause C.1 can be readily extended to an arbitrary transport network topology where a set of R radio sites $A_1, A_2, A_3, \ldots, A_R$ are connected to a common aggregation point C via cascades of multiple links, as illustrated in figure C.3. In this generalized scenario, a set of inequalities analogous to those derived for the four-site topology in figure C.1 can be obtained by systematically applying the BTA apportionment rule to every individual path from each radio site to the aggregation node C, regardless of the number or arrangement of intermediate links.

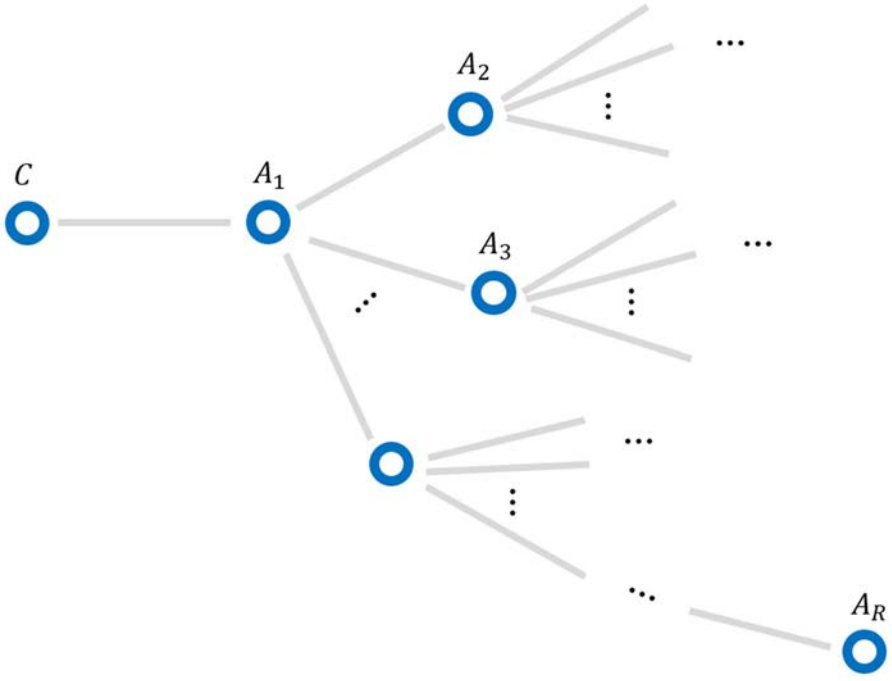

Figure C.3: Generalized transport network topology

History

Version	Date	Status
V1.1.1	March 2026	Publication